الجمهورية الجزائرية الديمقراطية الشعبية

République Algérienne Démocratique et Populaire

Ministère de l'Enseignement Supérieur
et de la Recherche Scientifique

وزارة التعليم العالي والبحث العلمي

Université Akli Mohand Oulhadj - Bouira -

Tasdawit Akli Muḥend Ulḥaǧ - Tubirett -

جامعة أكلي محند أولحاج
- البويرة -

Faculté des Sciences et des Sciences Appliquées

كلية العلوم والعلوم التطبيقية

Référence : ………………/MM/2021

المرجع:……./م م/ 2021

Mémoire de Master

Présenté au

Département : Génie Électrique

Domaine : Sciences et Technologies

Filière : Electrotechnique

Spécialité : Electrotechnique Industrielle

Réalisé par :

Wail Abid et **Imad Madoui**

Thème

Optimization of Optimal Power Flow Problem in Hybrid Power Systems involving Solar, Wind and Hydropower Plants Using Circulatory System-Based Optimization

Soutenu le **03 Juillet 2023** Devant la commission composée de :

Mr.:	MELLAH Hacene	M.C.A	Univ. Bouira	Président
	MOUASSA Souhil	M.C.A	Univ. Bouira	Rapporteur
	MADI Saida	M.C.B	Univ. Bouira	Examinateur

Année Universitaire : 2022-2023

الجمهورية الجزائرية الديمقراطية الشعبية
République Algérienne Démocratique et Populaire

وزارة التعليم العالي و البحث العلمي
جامعة أكلي محند أولحاج - البويرة

Ministère de l'Enseignement Supérieur
et de la Recherche Scientifique
Université Akli Mohand Oulhadj - Bouira
Tasdawit Akli Muhend Ulhağ - Tubirett

نموذج التصريح الشرفي الخاص بالالتزام بقواعد النزاهة العلمية لإنجاز بحث.

انا الممضي اسفله،

السيد(ة)عبيد وائلالصفة: طالب،

الحامل(ة) لبطاقة التعريف الوطنية:120347500

والصادرة بتاريخ2021/04/17

المسجل(ة) بكلية :**العلوم و العلوم التطبيقية**. قسم:.M2EIالهندسة الكهربائية

والمكلف(ة) بإنجاز اعمال بحث(مذكرة ماستر).

عنوانها:

Optimization of Optimal Power Flow Problem in Hybrid Power System Involving Solar, Wind and Hydropower Plant Using Circulatory System-based Optimization.

تحت إشراف الأستاذ(ة): مواسة سهيل

أصرح بشرفي اني ألتزم بمراعاة المعايير العلمية والمنهجية الاخلاقيات المهنية والنزاهة الاكاديمية المطلوبة في انجاز البحث المذكور أعلاه.

التاريخ:2023/07/03

توقيع المعني(ة)

رأي هيئة مراقبة السرقة العلمية:

النسبة:itin

% 12

الامضاء:

الجمهورية الجزائرية الديمقراطية الشعبية
République Algérienne Démocratique et Populaire

Ministère de l'Enseignement Supérieur
et de la Recherche Scientifique
Université Akli Mohand Oulhadj - Bouira
Tasdawit Akli Muhend Ulhağ - Tubirett

وزارة التعليم العالي و البحث العلمي
جامعة أكلي محند أولحاج - البويرة

نموذج التصريح الشرفي الخاص بالالتزام بقواعد النزاهة العلمية لإنجاز بحث.

انا الممضي اسفله،

السيد(ة)....مانوي عماد........الصفة: طالب، استاذ، باحث ....طالب.........

الحامل(ة) لبطاقة التعريف الوطنية: ...11551337.........والصادرة بتاريخ..29.08.2019

المسجل(ة) بكلية :العلوم و العلوم التطبيقية.......... قسم:..M.E.I الهندسة الكهربائية..........

والمكلف(ة) بإنجاز اعمال بحث(مذكرة، التخرج، مذكرة ماستر، مذكرة ماجستير، اطروحة دكتوراه).

عنوانها: optimization of optimal power flow problem in hybid power system involving solar, wind and hydropower plant using circulatory system based optimization.

تحت إشراف الأستاذ(ة): ....هواسة سهيل........................

أصرح بشرفي اني ألتزم بمراعاة المعايير العلمية والمنهجية الاخلاقيات المهنية والنزاهة الاكاديمية المطلوبة في انجاز البحث المذكور أعلاه.

التاريخ:...2023/07/03.......

توقيع المعني(ة)

رأي هيئة مراقبة السرقة العلمية:

النسبة: itin | % 10

الامضاء:

Author's Declaration

This is to certify that M.Wail Abid and Imad Madoui, Univ / Bouira- Ju 03, 2023 under the supervision of Dr. Souhil MOUASSA, conducted the research work presented in this thesis, entitled “Optimization of Optimal Power Flow Problem in Hybrid Power Systems involving Solar, Wind and Hydropower Plants Using Circulatory System-Based Optimization’’. No part of this thesis has been submitted anywhere else for any other degree. This thesis is submitted to the Department of Electrical Engineering, University Akli Mohand Oulhadj Bouira, Algeria, in the partial fulfilment of the requirement for the master's degree in industrial electrical engineering

ACKNOWLEDGEMENTS

We would like to begin by expressing our deepest gratitude to ALLAH, the source of all inspiration and guidance, for granting us the strength and perseverance to successfully complete this Master's thesis.

Our gratitude also extends to our family, which has been an unwavering support throughout this experience. Their love, encouragement, and constant support have been sources of inspiration and motivation that have contributed to our success.

We would also like to express our appreciation to our supervisor, Mr. MOUASSA SOUHIL, for his invaluable guidance, expertise, and support throughout this research. His insightful advice, availability, and dedication have been instrumental in the completion of this thesis.

Furthermore, we would like to extend our gratitude to all those who have contributed, directly or indirectly, to this research and our academic development. Their ideas, suggestions, and collaboration have enriched our work and contributed to its improvement.

Our thanks also go to those who have shared their knowledge, experience, and support during this journey. Their contribution has been invaluable and has greatly contributed to our growth as researchers.

In conclusion, this Master's thesis would not have been possible without the benevolent presence of God, the unwavering support of our family, and the attentive guidance of our supervisor. Their contribution has been of utmost importance.

Table of contents

Chapter 3: Solution of OPF Problems in Modern Power Systems

List of figures

List of tables

List of abbreviations

AEO	Artificial Ecosystem Optimizer
BMO	Barnacles Mating Optimizer
BWOA	Black Widow Optimization Algorithm
GTO	Gorilla Troops Optimizer
HS	Harmony Search
INFO	Weighted Mean of Vectors
MFO	Moth Flame Optimization
OPF	Optimal Power Flow
PDF	Probability Density Functions
POZs	Prohibited Operating Zones
PSO	Particle Swarm Optimization
PV	Photovoltaic
RESs	Renewable Energy Sources
CSBO	Circulatory System-Based Optimization
IEEE	Institute of electrical and electronics engineers

List of acronymes

- ai , bi , ci , di and ei : cost coefficients of ith generator
- αi , βi , γi , ωi and μi :emission coefficients of ith generator
- B_{ij} :susceptance at the transmission line i-j
- Cost_{PSH}:penalty cost for underestimation of combined solar and mini hydro power generations
- $\mathrm{Cost}_{PS,k}$:penalty cost for underestimation of kth solar power generation
- $\mathrm{Cost}_{PW,j}$penalty cost for underestimation of jth wind power generation
- Cost_{SHG}direct cost for combined solar PV and small hydro power unit
- $\mathrm{Cost}_{S,K}$direct cost of solar power
- $\mathrm{Cost}_{W,J}$direct cost of wind power
- Cost_{RSH}reserve cost of combined solar PV and small hydro power generation
- $\mathrm{Cost}_{RS,k}$reserve cost of solar power generation
- $\mathrm{Cost}_{RW,j}$reserve cost of wind power generation
- c_t carbon tax
- E ($P_{\mathrm{Sav,k}} < P_{\mathrm{SG,k}}$) expectation of solar PV power below $P_{\mathrm{SG,k}}$
- E ($P_{\mathrm{SHav}} < P_{\mathrm{SHG}}$) expectation of solar PV and small hydro power below $PSHG$
- F_{CE}total real cost and emission
- F_{Cost} total cost that include the valve loading effects $FEmission$ total emission
- F_{Loss} total real power loss in the transmission system
- F_{SHG} ($P_{\mathrm{SHav}} < P_{\mathrm{SHG}}$) probability of combined solar and mini hydro power shortage occurrence than the scheduled power
- f_s ($P_{\mathrm{Sav,k}} < P_{\mathrm{SG,k}}$) probability of solar power shortage occurrence than the scheduled power fW (pW ,j) wind power probability density function for jth wind power plant
- Gij conductance at the transmission line i-j

General introduction

GENERAL INTRODUCTION

The optimal power flow (OPF) problem is recognized as one of the most crucial challenges in the power system. It is a nonlinear, non-convex and large-scale issue. It entails satisfying operational, physical, and security constraints while simultaneously optimizing multiple objective functions. The task involves selecting suitable values for control variables to achieve the desired optimization outcome. The primary objective of OPF is to minimize the generation cost, power loss, emission…etc [1].

Due to the rising energy consumption and the high cost of producing energy through thermal generators. the world has been compelled to transition towards the inclusion of renewable energy sources in the electric grid, which in turn is considered clean, environmentally friendly and inexpensive. However, the integration of renewable energies into the electrical network has introduced complexity to the study of the optimal power flow (OPF) problem due to the intermittent nature of these sources. The primary objective of integrating renewable generators such as wind turbines, solar photovoltaic systems, and small hydro-power plants into the grid is to achieve several benefits. These include minimizing the generation fuel cost, reducing power losses, and mitigating environmental pollution [2].

Many methods and algorithms have been used for solving the OPF problem in the power system, using traditional mathematical algorithms or metaheuristic approaches. Among the classical optimization techniques are Newton method interior point and non-linear programming methods. It is undeniable that some of the algorithms mentioned above possess notable strengths, including excellent convergence properties and widespread utilization in industrial applications. However, It shows weaknesses that cannot be overlooked because it leads to a reduction in its efficiency [3].

In recent times, the use of metaheuristic algorithms has become more common, particularly in addressing the OPF problem. This is attributed to their ability to escape local optimality by leveraging simple principles inspired by nature. Various metaheuristic optimization techniques have been employed to solve the classical OPF problem, including improved versions of Particle Swarm Optimization (PSO) and the application of Moth Swarm Optimization (MSO). These metaheuristic approaches offer alternative and effective solutions to the OPF problem. Despite this, the use of the mentioned algorithms was limited in traditional power systems that contain only thermal power generators [4]

In recent years, researchers have conducted studies to address the optimal power flow (OPF) problem in hybrid power systems that incorporate both classical and renewable energy sources such as wind, solar, and hydropower [5]. These studies have involved the utilization of probability density functions (PDF), such as Weibull and log normal distributions, to forecast variables like wind speed and solar irradiance. These probabilistic models enable researchers to incorporate the uncertainty and variability associated with renewable energy sources into the OPF problem formulation [6].

In this thesis, IEEE 30-bus and IEEE 57-bus test systems are modified in order to integrate solar, wind and small-hydro power generators with a limited number of thermal generators. The uncertainties of wind speed, solar irradiance and river flow are treated in detail and are modeled using probability density functions, namely Weibull, log normal and Gumbel respectively. Two distinct scenarios are considered in this research to address the intermittency of renewable sources: overestimation and underestimation. To account for these scenarios, both reserve and penalty costs are included in the generation cost.

This study presents the application of the Circulatory System-Based Optimization algorithm (CSBO) to solve the OPF problem. It is important to note that this application of the CSBO algorithm to the OPF problem, considering these specific renewable energy sources, has not been documented in the existing literature. Thus, this study represents the first-ever attempt to utilize the CSBO algorithm for addressing the OPF problem in this context.

The rest of the thesis will be structured as follows:

In the first chapter, we will present the description of the power flow and optimal power flow problems, as well as the main objective and the formulation of the power flow (PF) and OPF problems. Then, we will discuss the optimization principles of classical methods and their limitations.

The second chapter will mainly focus on meta-heuristic optimization methods, first we will focus on defining what's a metaheuristic optimization method is, followed by detailed presentation of the proposed algorithm CSBO (definition, inspiration, mathematical equations and so on). Lastly, we briefly presented three other algorithms (PSO, MFO and BWOA) that will be used in the third chapter along with other algorithms when comparing the obtained results from the application of CSBO.

The third chapter, in its first part, will provide a small introduction to the OPF problem involving wind turbines, solar photovoltaic (PV), and small hydropower. Then, the problem formulation is described along with the description of the different objective functions and the Modeling of the Uncertainty of Renewable Energy Generators, while also providing the parameters of the studied

IEEE 30-bus and IEEE 57-bus networks. In the second part of this chapter, the proficiency of the proposed CSBO algorithm was authenticated by comparing its results with those of other contemporary optimizers. It was observed that the proposed method consistently yielded a better optimal cost for various objective functions, outperforming the other optimizers.

Finally, we will conclude this modest thesis with a general conclusion on our effective contribution and positive impact in the integration of renewable energies into electrical networks.

Chapter 1: Optimal Power Flow (OPF) Problem

Chapter 1:
OPTIMAL POWER FLOW PROBLEM

1.1.Introduction

The optimal power flow (OPF) is one of the most studied nonlinear optimization problems. The OPF's goal to optimize the production and transmission of electrical energy in distribution networks while considering system constraints and control limits. There is a wide diversity of OPF formulations and solution methods available in the literature survey. The nature of the OPF continues to change due to the modernization of electricity markets and the addition of renewable resources [7].

In this chapter, we present power flow and its variables, as well as the formulation of the problem using the Newton-Raphson method. We also discuss the categorization of variables and constraints and the construction of the objective function. Finally, we provide a summary of the formulation of the optimal power flow.

1.2.Power flow (load flow) definition and objective

The power flow problem (load flow) study in an electrical network refers to the analysis and calculation of the variables of an electric network under normal balanced operation in steady state. These variables include node voltages, injected powers at nodes, and power flows in the lines. Losses and currents can be derived from these variables.in a given network. So, in simpler language we can say It involves studying and analyzing the flow of electrical power from sources (the generation sources such as power plants) through the transmission and distribution networks to the numerous loads (consumers) linked to the system [8].

The study of power flow involves calculating the voltage values within an electrical network at specified ends and given conditions at bus sets. From these voltages, the active and reactive powers flowing through each line and transformer are calculated. The set of equations representing the electrical network is nonlinear in nature.

In practical applications, power flow calculation methods utilize the network configuration and equipment properties to determine the complex voltage at each node. Additionally, these methods assume perfect symmetry between the three phases of the three-phase system in the electrical network. By considering these factors, an accurate assessment of the voltage conditions within the network can be obtained [9]

Power flow studies are used for planning the construction and expansion of electrical networks, as well as their operation and control. The result of a power flow problem informs the operator or network planner about how the network lines are loaded, what the voltages are at different bus sets, how much generated power is lost, and where the limits are exceeded [10].

In power flow calculation, a bus bar is defined by four parameters which are classified as given in the following subsection.

*1.2.1.*Classification of bus bars according to their specifications [9]

We can classify bus bars into three categories based on the specifications of the variables used.

For each bus bar, two variables need to be specified beforehand, and the other two variables are to be calculated.

- Reference bus bar (slack bus): It is a generator bus bar that can be classified based on two specified variables: the voltage magnitude (V) and the phase angle (δ). The power values (P and Q) at this bus bar are initially unknown and need to be determined through calculations.

To establish a reference point for voltage angles, the reference bus bar is selected from the generator bus bars with the highest active power. This reference bus bar serves as the benchmark for determining the voltage angles at other bus bars in the system.

- Load bus bar: This bus bar supplies a load characterized by its active power P and reactive power Q. Therefore, (P, Q) are specified, while (V, δ) are to be calculated.

- Generator bus bar: This bus bar is connected to a generator that delivers an active power P under a constant voltage V controlled by an Automatic Voltage Regulator (AVR). Therefore, (P, V) are specified, while (Q, δ) are to be calculated.

Table 1 : Classification of bus bars according to their specifications [9]

Types of bus bars	**Known variables**	**Unknown variables**
Reference bus bar (V $\boldsymbol{\delta}$)	V, $\boldsymbol{\delta}$	P, Q
Generator bus bar (PV)	P, V	Q, $\boldsymbol{\delta}$
Load bus bar (PQ)	P, Q	V, $\boldsymbol{\delta}$

1.2.2.Formulation of power flow equations [11].

The study of power flow involves calculating the voltages of the electrical network for specified endpoints and given conditions at the buses, such as capacitive or inductive loads that need to be supplied, generated powers, and voltage magnitudes at all buses. From these values, the currents in the transmission lines, power flows, and power losses can be obtained. The nodal currant and voltage equations of an electrical network with N buses are written in the following matrix form:

Equation (1.1) gives the relationship between the current and the voltage in an electrical network. So we can say:

The nodal currant - voltage equation of an electrical network with N buses is given by the following equations.

$$\begin{bmatrix} I_1 \\ I_2 \\ \vdots \\ I_N \end{bmatrix} = \begin{bmatrix} Y_{11} & Y_{12} & \cdots & Y_{1N} \\ Y_{21} & Y_{22} & \cdots & Y_{2N} \\ \vdots & \vdots & \ddots & \vdots \\ Y_{N1} & Y_{N1} & \cdots & Y_{NN} \end{bmatrix} * \begin{bmatrix} V_1 \\ V_1 \\ \vdots \\ V_1 \end{bmatrix} \quad (1.\ 1)$$

Where:

$$I_{BUS} = Y_{BUS} * V_{BUS} \quad (1.\ 2)$$

$I_{BUS} = [I_1, I_2, \ldots I_N]^{\mathrm{T}}$: The vector of injected currents into each bus bar represents the external source current. The current flowing from bus bar i to bus bar j is considered positive, while the current flowing in the opposite direction is considered negative.

$V_{BUS} = [V_1, V_2, \ldots V_N]^{\mathrm{T}}$: The vector of complex voltages at each bus bar and Y_BUS represents the admittance matrix of the system, which has a size of (N * N), where N is the number of bus bars in the system.

Y_{ii} : The diagonal element of the admittance matrix represents the sum of all the components connected to that particular bus bar. This can be expressed mathematically by the following equation:

$$Y_{ii} = \sum_{\substack{i=0 \\ i \neq k}}^{N} y_{ik} \quad (1.\ 3)$$

y_{ik} : The off-diagonal element i, k of the admittance matrix represents the negative sum of all the components connected between bus bar i and bus bar j. In other words, it can be expressed as follow:

$$Y_{ik} = -\sum_{k \neq i} y_{ik} \quad (1.\ 4)$$

According to equation (1.1), the net injected current at bus bar i can be expressed as follows:

$$I_1 = \sum_{k=1}^{N} Y_{ik} * V_k \ \ for \ \mathrm{i} = 1, 2 \ldots., \mathrm{N} \quad (1.5)$$

Where:

$$\bar{Y}_{ik} = G_{ik} + j * B_{ik} = Y_{IK}(cos\delta_{ik} + jsin\delta_{ik}) \quad (1.6)$$

$$\bar{V}_k = R_{Ek} + j * Im_k = V_K(cos\delta_k + jsin\delta_k) \quad (1.7)$$

G_{ik} and B_{ik} are the conductance and susceptance of $\bar{Y}_{ik}$; R_{Ek} and Im_k respectively the real and imaginary parts of $\bar{V}_k$ respectively. δ_k is the phase of the voltage at the busbar k;

δ_{ik} : the phase of the element ik;

The expression of the injected apparent power $\bar{S}_i$ at a bus bar can be written as given by the following equation:

$$S_i^* = P_i - Q_i = V_i^* * \sum_{k=1}^{N} \bar{Y}_{ik} * \bar{V}_k \quad (1.8)$$

$\bar{P}_i$,$\bar{Q}_i$: where $\bar{P}_i$ and $\bar{Q}_i$ are the active and reactive powers at bus bar I, respectively. By substituting equations (1.5) and (1.6) into equation (1.7), we obtain the following equation:

$$P_i = \sum_{k=1}^{N} V_i V_k Y_{ik} \cos(\delta_{ik} + \delta_k - \delta_i) \quad i = 1,2, \ldots, N \quad (1.9)$$

$$Q_i = \sum_{k=1}^{N} V_i V_k Y_{ik} \sin(\delta_{ik} + \delta_k - \delta_i) \quad i = 1,2, \ldots, N \quad (1.10)$$

The equations (1.9) and (1.10) represent the power flow equations as follows:

$$P_i = P_{Gi} + P_{Di} \quad (1.11)$$

$$Q_i = Q_{Gi} + Q_{Di} \quad (1.12)$$

Where P_{Gi} and Q_{Gi} are generated the active and reactive powers generated, respectively.
P_{Di} and Q_{Di} are the active and reactive powers demanded at the bus i, respectively .
Figure 1.1. represents the flowchart of Newton Raphson method

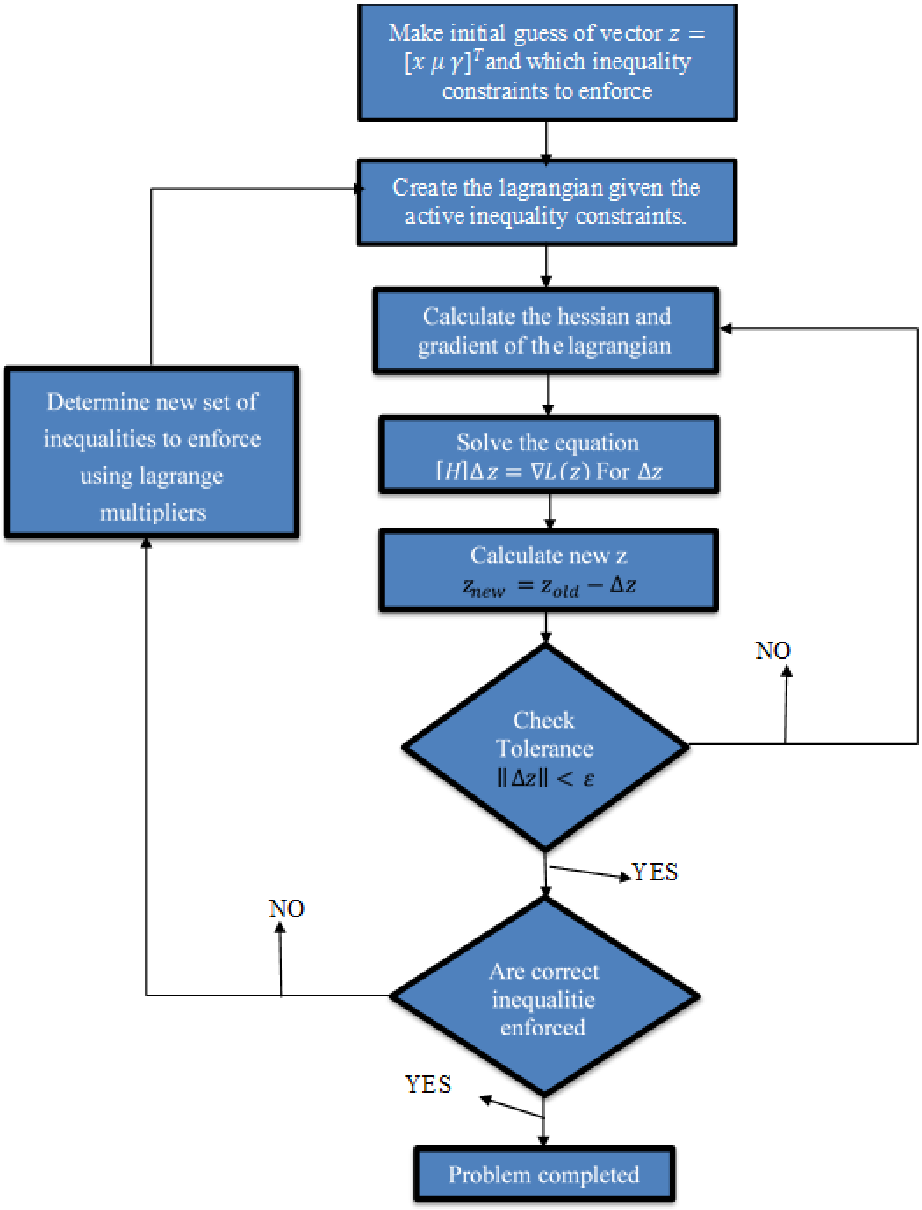

Figure 1-1: Newton Raphson method's flowchart [12].

1.2.3.Power flow problem solution methods

Generally, the method used to solve the problem flow problem is Newton-Raphson due to its fast convergence and reduced number of iterations compared to other methods (such as Gauss-Seidel). The Taylor series expansion of equations (1.8) and (1.9) is given by the following equation:

$$\begin{bmatrix}\Delta P\\ \Delta Q\end{bmatrix} = J * \begin{bmatrix}\Delta \theta\\ \Delta Q\end{bmatrix} \Rightarrow \begin{bmatrix}\Delta P\\ \Delta Q\end{bmatrix} = \begin{bmatrix}J_1 & J_2\\ J_3 & J_4\end{bmatrix} * \begin{bmatrix}\Delta \delta\\ \Delta v\end{bmatrix} \tag{1. 13}$$

$$J_1 = \frac{\partial P_i}{\partial \delta_K}, J_2 = \frac{\partial P_i}{\partial V_K}, J_3 = \frac{\partial Q_i}{\partial \delta_K}, J_4 = \frac{\partial V_i}{\partial V_K} \tag{1. 14}$$

Where: ΔP and ΔQ represent the differences between the specified and calculated active powers, and the differences between the specified and calculated reactive powers, respectively.

Δδ and Δv represent the differences between the specified and calculated angles, and the differences between the specified and calculated voltages respectively. J is the Jacobian matrix.

$$\Delta \mathrm{P}_i = P_i^{spé} - P_i^{cal} \tag{1. 15}$$

$$\Delta \mathrm{Q}_i = Q_i^{spé} - Q_i^{cal} \tag{1. 16}$$

For a network with N buses, with NG generator buses, there are 2(N - 1) - NG equations to solve. Consequently, there are (N - 1) equations for active power and (N - 1 - NG) equations for reactive power, resulting in a Jacobian matrix of size (2N - 2 - NG) x (2N - 2 - NG) elements.

The calculation of the Jacobian matrix elements is done as follows: [11]

The diagonal and off-diagonal elements of J1 are given by the following equation:

$$\frac{\partial P_i}{\partial \delta_i} = \sum_{k\neq 1} |V_k||Y_{ik}||V_i| \sin(\delta_{ik} + \delta_k - \delta_i) \tag{1. 17}$$

$$\frac{\partial P_i}{\partial \delta_k} = -|V_k||Y_{ik}||V_i| \sin(\delta_{ik} + \delta_k - \delta_i) \quad K \neq i \tag{1. 18}$$

The diagonal and off-diagonal elements of J2 are given by the following equation:

$$\frac{\partial P_i}{\partial V_i} = 2|Y_{ii}||V_i| \cos(\delta_{ii}) + \sum_{k\neq 1} |V_k||Y_{ik}||V_i| \cos(\delta_{ik} + \delta_k - \delta_i) \tag{1. 19}$$

$$\frac{\partial P_i}{\partial V_i} = |V_{ij}||V_i| \cos(\delta_{ik} + \delta_k - \delta_i) \quad \mathrm{K} \neq \mathrm{i} \tag{1. 20}$$

The diagonal and off-diagonal elements of J3 are given by the following equation:

$$\frac{\partial Q_i}{\partial \delta_i} = \sum_{k\neq 1} |V_k||Y_{ik}||V_i| \cos(\delta_{ik} + \delta_k - \delta_i) \tag{1. 21}$$

$$\frac{\partial Q_i}{\partial V_i} = -2|Y_{ii}||V_i| \sin(\delta_{ii}) + \sum_{k\neq 1} |V_k||Y_{ik}||V_i| \sin(\delta_{ik} + \delta_k - \delta_i) \tag{1. 22}$$

The diagonal and off-diagonal elements of J4 are given by the following equation:

$$\frac{\partial Q_i}{\partial V_i} = -2|Y_{ii}||V_i| \sin(\delta_{ii}) + \sum_{k\neq 1} |V_k||Y_{ik}||V_i| \sin(\delta_{ik} + \delta_k - \delta_i) \tag{1 .23}$$

$$\frac{\partial Q_i}{\partial V_k} = -|V_k||V_i|\sin(\delta_{ik} + \delta_k - \delta_i) \quad K \neq i \tag{1 .24}$$

1.3. Optimal Power Flow (OPF)

Optimal Power Flow (OPF) is a mathematical optimization problem in the field of electrical power systems. It is widely regarded as a fundamental tool in this field and has been the subject of wide research since it was introduced by *Carpentier* in 1962. The objective of the OPF problem is to identify the optimal settings for a given power system network in order to optimize a specific objective function while satisfying the power flow equations, system security, and operational limits of equipment. This involves manipulating various control variables, including generator real power outputs, voltages, transformer tap settings, phase shifters, switched capacitors, and reactors, to achieve an optimal network configuration based on the defined problem formulation. Moreover, OPF can offer valuable support to operators in addressing various challenges encountered in the planning, operation, and control of power networks.

The primary objective of OPF is to minimize a cost function or maximize a performance index while ensuring that the power system operates within specified limits. The performance index can be related to efficiency, voltage stability, system reliability, or any other desired system performance parameter. The most utilized objective function in OPF is the minimization of overall fuel cost. However, other traditional objectives such as minimizing active power loss, bus voltage deviation, emissions from generating units, the number of control actions required, and load shedding. With the deregulation of the electric power industry. One of the major challenges in the OPF problem lies in the nature of the control variables, as some are continuous (such as real power outputs and voltages), while others are discrete (such as transformer tap settings, phase shifters, and reactive injections).

The application domains of optimal power flow can be classified as follows [13–15]

- Minimization of fuel cost.
- Minimization of losses.
- Improvement of voltage profile and stability.
- Maximization of power transfer capability

1.3.1.Problem formulation of optimal power flow model [16].

The main objective in solving OPF problems is to identify the optimal values for control variables, which involves minimizing a specific objective function while adhering to all physical and security constraints. Mathematically, the OPF problem can be expressed as follows:

$$\text{Minimize:} \quad f(x,u) \tag{1.25}$$

Subject to:

$$\mathrm{g}(x,u) = 0 \tag{1. 26}$$

$$\mathrm{h}(x,u) \leq 0 \tag{1. 27}$$

where:

f(x,u) presents the objective function;

x represents the state variables vector of a power system network;

u represents the control variables vector;

$g(x,u)$ represents the equality constraints;

$h(x,u)$ represents inequality constraints, where, $h_{\max}$ and $h_{\min}$ are the upper and lower boundary limits, respectively .

1.3.2.Optimal power flow variables classification [15]

In optimization problems, two main types of variables are considered: independent variables, also known as control or decision variables, and dependent variables, also known as state variables. The optimization process involves first determining the optimal values for the control variables and then calculating the corresponding values for the state variables based on those optimal control values.

In the OPF problem, control variables may include:

- Active power generation of all generator buses except slack bus;
- Voltage of all generator buses;
- Tap setting of all transformers;
- Reactive power injection of shunt capacitor banks;
- Moreover, state variables may also include;
- Active power output of the slack bus;
- Load bus voltages ;
- Reactive power generation of generators;
- Transmission line loadings.

It is important to note that the number of control variables determines the dimensionality of the solution space. In other words, a problem with n control variables will result in an n-dimensional solution space.

1.3.3. Constraints formulation

OPF Constraints in the OPF problem are typically classified into two types: equality constraints and inequality constraints. These conditions define the feasible region of the problem, and any solution must fall within this region in order to satisfy all the constraints.

1.3.3.1. Equality constraints

The equality constraints in load flow analysis are derived from the physical laws that govern the behavior of an electrical network. These constraints are expressed as nonlinear equations in the power flow equations, which ensure that the net injection of active and reactive powers at each bus is equal to zero.

$$\begin{cases} P_{Gi} - P_{di} - V_i \sum_{j=1}^{NB} V_j \left[G_{ij}\cos(\delta_{ij}) + B_{ij}\sin(\delta_{ij}) \right] = 0 \\ Q_{Gi} - Q_{di} - V_i \sum_{j=1}^{NB} V_j \left[G_{ij}\sin(\delta_{ij}) - B_{ij}\cos(\delta_{ij}) \right] = 0 \end{cases} \tag{1.28}$$

Where:

NB is the total number of busses of the power system;

P_{Gi} is the active power of generation;

Q_{Gi} is the reactive power of generation;

P_{di} is the active power of demand;

Q_{di} is the reactive power of demand;

G_{ij} the conductance of the corresponding lines between the (i, j) buses;

B_{ij} the susceptance of the corresponding lines between the (i, j) buses.

1.3.3.2. Inequality constraints

In the context of the OPF problem, inequality constraints typically impose limitations on various physical components in the electrical system. These components can include generators, tap-changing transformers, and phase-shifting transformers. Additionally, system security requirements and reactive power compensation limits contribute to the set of inequality constraints. Specifically, when considering generators, these constraints are concerned with maintaining active and reactive power levels within acceptable boundaries.

$$P_{Gi}^{min} \leq P_{Gi} \leq P_{Gi}^{max} \tag{1. 29}$$

$$Q_{Gi}^{min} \leq Q_{Gi} \leq Q_{Gi}^{max} \tag{1 .30}$$

The inequality constraints for load tap-changing transformers involve maximum and minimum tap positions, which determine the voltage level relative to the nominal voltage. These constraints are utilized to adjust voltage magnitudes and regulate reactive power flows. On the other hand, phase-shifting transformers have maximum and minimum phase angle shifts to control voltage phases and regulate active power flows. These specific constraints are considered for both types of transformers.

$$T_{ik}^{min} \leq T_{ik} \leq T_{ik}^{max} \tag{1 .31}$$

$$\alpha_{ik}^{min} \leq \alpha_{ik} \leq \alpha_{ik}^{max} \tag{1. 32}$$

Reactive power compensators such as Batteries, reactors, etc. have limits defined by minimum and maximum values, which determine their operating range. These limits ensure that the devices operate within acceptable bounds and can effectively compensate for reactive power in the system.

$$Q_{Ci}^{min} \leq Q_{Ci} \leq Q_{Ci}^{max} \tag{1 .33}$$

Bounds on the apparent power flow in power transformers and transmission lines are set to uphold network security and avoid issues such as instability or thermal losses in conductors. These limits ensure that the power flow in these components remains within safe operating conditions, avoiding excessive heating and potential damage to the system.

$$|S_{ik}|^2 \leq |S_{ik}^{max}|^2 \tag{1. 34}$$

To preserve the quality of system security and electrical service, it is essential to limit violations on voltage constraints, which must remain within their tolerable limits.

$$V_i^{min} \leq V_i \leq V_i^{max} \tag{1. 35}$$

1.3.3.3.Handling constraint [14].

There are different ways to handle constraints in evolutionary computation optimization algorithms.

- Preserving feasible solution method;
- Solution repair method;
- Infeasible solution rejection method;
- Penalty function method

1.3.4. Objective functions

In optimal power flow (OPF), the objective function signifies the objective or target to be reached when optimizing the operation of a power system. The objective function is usually defined mathematically and measures the system's performance or cost.

Typically, the most commonly utilized objective in the OPF problem formulation is the minimization of the overall cost associated with the active power generation from real energy production units. The cost of each production unit is assumed to be solely dependent on the active power generated and is represented by quadratic curves. Consequently, the total objective function of the electrical system can be expressed as the sum of the quadratic cost models for all generators involved. By minimizing this objective function, the OPF algorithm aims to optimize the operation of the system by determining the optimal values for the control variables that minimize the total generation cost.

Minimise

$$F = \sum_{i=1}^{NG} f_i = \sum_{i=1}^{NG} a_i P^2 + b_i P_i + c_i \ \left(\frac{\$}{\mathrm{h}}\right) \quad (1.\ 36)$$

or

$$P_{Gi\,min} \leq P_{Gi} \leq P_{Gi\,max} \quad (1.\ 37)$$

$$P_{Di} = P_{Gi} + P_{Li} \quad (1\ .38)$$

Where ai, bi, ci signify the cost coefficients of the i-*th* generation unit, and PDi, PLi are the demanded power and the active transport losses, respectively.

1.3.5.Classical methods applied to the optimal power flow problem [17]

There are several classical optimization techniques that have been applied to solve Optimal Power Flow (OPF) problems. Here are six categories of these techniques, along with a brief description of each and their application statistics:

- **Newton's method**: in general, these are nonlinear equations that need to be solved using iterative methods. The Newton method is particularly preferred because of its quadratic convergence properties.

- **Linear programming**; Linear programming is a mathematical optimization technique used to solve problems that involve linear constraints and an objective function. In this method, both the objective function and constraints are represented as linear equations or inequalities, and the variables are required to be non-negative.

- **Quadratic programming**; Quadratic programming is a specific type of nonlinear programming where the objective function is quadratic, and the constraints are either linear or linearized.
- **Nonlinear programming**: Nonlinear programming (NLP) is a branch of optimization that focuses on solving problems with nonlinear objective functions and constraints. In NLP, the constraints can be either from equalities or inequalities or both. The inequality constraints can be bounded, meaning they have specified upper and lower limits. This allows for more flexibility in defining the feasible region and finding optimal solutions.

- **Interior point method**: The interior point method, which has recently been rediscovered, offers a faster and potentially superior alternative to the conventional simplex algorithm for solving linear programming problems. Furthermore, this method has been extended to tackle nonlinear programming (NLP) and quadratic programming (QP) problems, showing remarkable qualities and yielding promising results. By introducing nonnegative slack variables, the interior point methods transform inequality constraints into equalities. A logarithmic barrier function, incorporating the slack variables, is subsequently added to the objective function, multiplied by the barrier parameter. Throughout the solution process, this parameter is gradually reduced to zero, ensuring convergence within the feasible region.

1.3.6.Limitations of Classical Search Methods

Addressing optimization problems using classical or traditional techniques can be challenging due to various factors depending on the nature of the problem. Difficulties arise when dealing with problems that have multiple local optima, involve discontinuities, exhibit changes in optimal solutions over time, or have constraints within the search space. Additionally, classical search techniques often struggle with problems that have large and complex exploration or search spaces, limiting their ability to thoroughly explore all potential solutions. Large-scale problems may be computationally expensive to solve using classical methods [18]. Overall, these limitations highlight the need for alternative approaches, such as metaheuristic optimization methods, in complex optimization scenarios. These methods will be discussed in the second chapter of this thesis.

1.4. Conclusion

In this chapter, we have presented the problem of ordinary power flow and optimal power flow, including its general formulation., discussed objective functions, and categorized the variables and constraints. It can be concluded that the study of power flow is fundamental to ensure safe, efficient, and reliable operation of electrical networks. Through a detailed analysis of power flow, operators can optimize network performance.

Chapter 2: Metaheuristic Optimization Methods

Chapter 2:
METAHEURISTIC OPTIMIZATION METHODS

2.1.Introduction

The optimal power flow problem is considered one of the most challenging and intriguing issues in power systems. It involves solving a constrained optimization problem that is characterized by non-linearity and non-convexity. Researchers have dedicated significant efforts over the past decades to develop optimal solutions for the OPF problem while ensuring system stability. [19]

Earlier, many classical (deterministic) optimization algorithms had been successfully applied to the optimal power flow problem. But due to the limitations and inconveniences of classical optimization methods such as the limits mentioned in the previous chapter. many metaheuristics have been developed and many of them have been used to solve the OPF problem.

It is important to note that there isn't a single algorithm that can solve all types of OPF problems effectively. The OPF problem can be formulated in different ways, with various objectives, variables, and constraints. This creates a need for new algorithms that can efficiently solve specific types of OPF problems this is known as The No Free Lunch Theorem (NFL theorem) In this chapter we will address three main points, which will be presented as follows. [20]

- An introduction to meta-heuristic optimization methods (definition, background, advantages. etc.).
- A detailed presentation of a new meta-heuristic algorithm inspired by regular body functions called CSBO.
- Information about some other algorithms that were used to solve similar OPF problems and chosen to compare with CSBO to further indicate its performance.

2.2. Metaheuristic optimization methods

Optimization techniques are applicable to a wide range of problems where the goal is to search for optimality. There are numerous ways to classify and name these problems and as a result, the techniques used for optimization can vary considerably from one problem to another. In short we can define Optimization techniques as mathematical tools that aid in selecting the best decision from the available set of possible solutions to achieve the optimal goal. After the problem variables are defined, [21].Various optimization techniques can be employed to solve the OPF problem. These techniques can be broadly classified into two categories: mathematical methods and heuristic approaches.

Mathematical methods involve the formulation of the problem using mathematical representations and equations.

Nevertheless, it is important to note that mathematical methods may not always be capable of solving highly complex problems effectively. [15]

2.2.1. Heuristics and metaheuristics

Heuristics are solution strategies or approaches that involves trial-and-error to generate satisfactory solutions to complex problems within a practical time frame, the degree of complexity of the treated problem can determine the chance to search every possible solution or combination, therefore the goal should be focused on finding good, feasible solutions in an acceptable timescale. [22]

2.2.1.1.Metaheuristics

A Meta-heuristic is a high-level heuristic technique that aims to provide a sufficiently good solution to an optimization problem, especially for spic-and-span information with unlimited computational power that cannot be solved by traditional means. [23]

Meta-heuristics, as high-level techniques, do not guarantee the attainment of a globally optimal solution in any problem space. This limitation is due to the stochastic nature of most global optimization te[2]chniques employed in metaheuristics. These techniques heavily rely on the utilization of random variables, which greatly influences the obtained solution. As a result, the solution achieved through metaheuristics is highly dependent on the specific random variables generated during the optimization process.

Meta-heuristics are indeed effective in tackling combinatorial optimization problems, often providing good solutions even with limited computational resources.in optimization algorithms, with a wide range of feasible solutions. They have been proven to be useful approaches for optimization problems. In other words, metaheuristics can be seen as modern, nature-inspired algorithms or global search techniques that are valuable tools for optimization.

These algorithms are highly effective and widely applicable, offering strong performance and a compelling drive towards achieving optimal solutions. In some cases, metaheuristic techniques are considered stochastic or fuzzy search methods that operate at a population level. When compared to direct search algorithms or classical gradient-based techniques, these techniques provide robust and high-level solutions. They belong to a higher class of algorithms that are designed to explore and search for good solutions to optimization problems. They achieve this by combining different concepts, perceptions, and ideas in order to strike a balance between exploiting known solutions and exploring new possibilities. Exploration involves delving into the search space to uncover new potential solutions, while exploitation focuses on refining the search process to find better solutions within the vicinity.

In simpler terms, metaheuristics are powerful algorithms that intelligently navigate the search space to find practical solutions for optimization problems. They blend different approaches to strike a balance between exploring new options and improving existing solutions. By doing so, they are able to uncover promising solutions and continuously refine the search process. [18]

2.2.1.2.Shared characteristics of deferent meta-heuristic optimization algorithms

- All meta-heuristic optimization algorithms share the same following characteristics.
- They are based on some fundamental theories and mathematical models.
- They are simple and easily implemented.
- It is easy to develop their variants based on the existing meta-heuristics.

They can be considered black boxes, from which, by given a set of inputs, a set of outputs can be easily obtained [15]Classification of metaheuristic optimization algorithms

There are different bases for the classification of metaheuristic optimization algorithms in the literature. Two main classifications are based on the number of random solutions it generates at each step and the algorithm's inspiration [24] .

The first classification separates the algorithms to two classes: [25].

Trajectory-based methods and population-based methods. The key distinction between these two classes is the number of tentative solutions used at each step of the iterative algorithm. Begin with a single initial solution. At each search step, the current solution is replaced by another solution found in its neighborhood, often the best one. Trajectory-based metaheuristic methods have a tendency to quickly identify a local optimal solution.

On the other hand, population-based algorithms operate on a population of candidate solutions. Initially, this population is generated randomly, and subsequently improved through an iterative procedure. During each iteration, certain individuals within the population are replaced with newly generated ones, typically chosen based on their suitability for the given problem. This process results in the formation of a new generation.

Figure 2-1 represents classification based on trajectory/population-based methods.

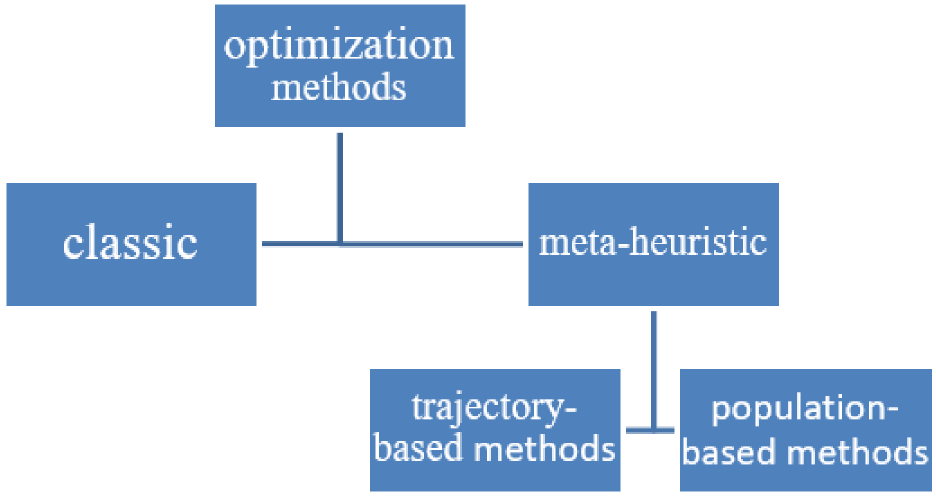

Figure 2-1 : Classification based on trajectory/population based methods

The inspired meta-heuristic algorithms are classified into four subclasses as a primary classification [24]

- Evolutionary techniques;
- Swarm intelligence techniques ;
- Physics-based techniques;
- Human-related techniques.

Figure 2-2 represents the classification of the inspired meta-heuristic algorithms.

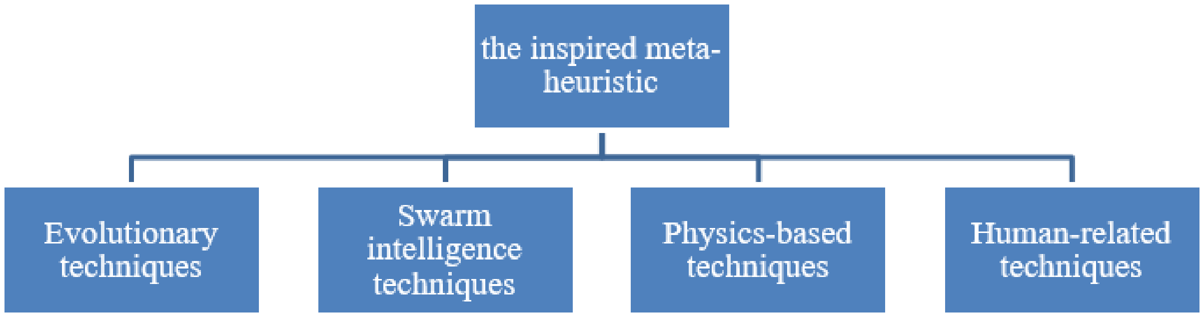

Figure 2-2 : Classification based on the inspiration of metaheuristic methods

2.3.Circulatory System Based Optimization (CSBO) algorithm [26]

CSBO is a new algorithm that draws inspiration from the regular functions of the human body. More specifically as its name suggest this algorithm is based on Regular circulatory system of humans.

2.3.1.Regular circulatory system

Blood plays a crucial role in maintaining the body's well-being, it transports oxygen and essential nutrients from the lungs to the body's tissues, it also facilitates the removal of waste products like carbon dioxide. This circulation of blood is vital for sustaining life and ensuring the overall health and proper functioning of all body parts. The body's blood vessels are functionally separated into two distinct circuits. Based on the simplistic model inspired by the circulatory system of the body, showed in Figure 2-3.

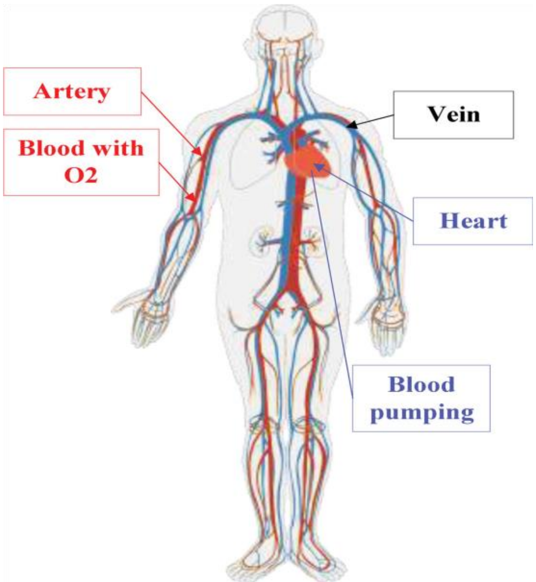

Figure 2-3 : A simple inspiration model from the circulatory system for modeling CSBO

The right ventricle serves as the pump for the pulmonary circuit, responsible for circulating blood through the lungs. On the other hand, the left ventricle acts as the pump for the systemic circuit, which supplies blood to the body's tissue cells. During pulmonary circulation, the oxygen-poor blood is transported from the right ventricle to the lungs, where it receives a fresh supply of oxygen. Subsequently, the oxygen-rich blood is returned to the left atrium.

Systemic circulation is responsible for supplying functional blood to all body tissues. It transports oxygen and nutrients to the cells while collecting carbon dioxide and waste products. Oxygenated blood is carried from the left ventricle through arteries to the capillaries in the body's tissues. Deoxygenated blood, on the other hand, returns from the tissue capillaries through a network of veins to the right atrium of the heart. It then moves into the right ventricle, completing one cycle, which is analogous to one iteration in our proposed algorithm.

Blood is classified as a Newtonian fluid. The primary variables associated with the circulatory system include flow, pressure, and volume. The modeling of pressure-flow within the circulatory system can be approached from two perspectives, beating and non-beating. The model in question is inspired by the beating perspective, focusing on the dynamic nature of the circulatory system.

2.3.2. Circulatory system regular performance as an intelligent systematic algorithm CSBO

The algorithm treats the pulmonary and systemic circuits as separate groups, each having its own distinct optimization cycle. These circuits can be seen as specific functions modeled on a specific type of population.

In the CSBO algorithm, similar to other metaheuristic optimization algorithms, an initial population is generated randomly within the problem range. This population represents the mass of blood droplets, and their positions correspond to potential solutions in the search space for the optimization problem. The circulatory system functions as an operator on this population, refining and strengthening the solutions while eliminating weaker individuals. In essence, the algorithm iteratively improves the quality of solutions (represented by blood) within the search space (represented by the body), inspired by the functionality of the circulatory system in the body.

Figure 2-4 illustrates how the evolutionary process of blood in the circulatory system can be modeled as an optimization system.

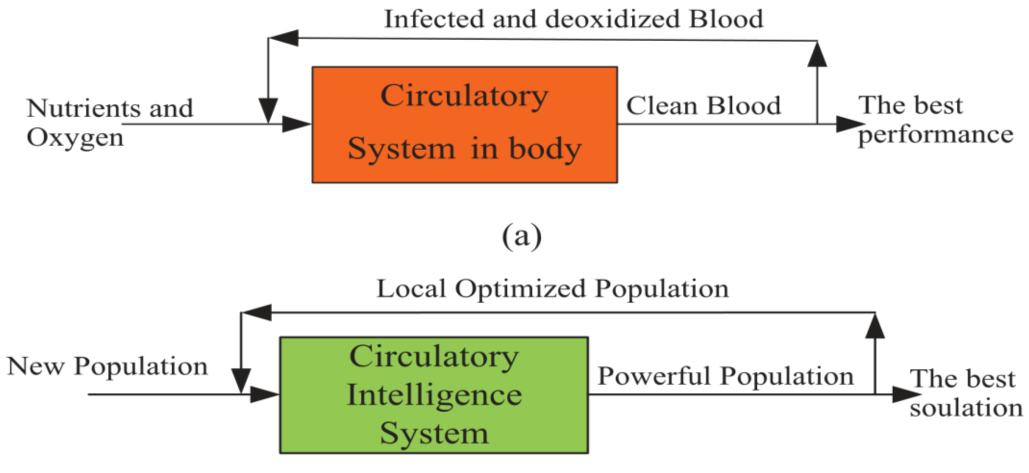

(a)

(b)

Figure 2-4: The blood circulatory (a) and equivalent optimizer (b) process

The pulmonary circulation handles the deoxygenated blood, which can be considered equivalent to the weaker population. Conversely, the systemic circulation deals with oxygenated blood, which represents the population with better target values or solutions. In other words, it deals with the stronger population, each blood mass (*BMi*) corresponds to an individual in the population. The movement of each BM_i is determined by its position, which directs it towards a more optimal position if possible, or it remains in its current position. Figure 2-4 illustrates how the evolutionary process of blood in the circulatory system can be modeled as an optimization system. **Table 2** represent The equivalent concepts of the circulatory system

Table 3 : The equivalent concepts of the circulatory system

Element or function in the circulatory system	The equivalent concept in the CSBO algorithm
Blood mass	Algorithm population
Blood movement in the body	Population movement within the problem range
Cleaner blood with more oxygen	Objective function
Circulation cycle	Algorithm iteration
Deoxygenated blood	Weaker population
Oxygenated blood	Stronger population
Blood purification	Population composition
Blood pumping	Changing the population position
CO_2 separation from blood	Crossover
Pulmonary and systemic circulations	Population separation

2.3.3.The mathematical modeling of the CSBO algorithm

The CSBO algorithm, similar to other metaheuristic algorithms, begins by generating an initial population or blood masses BMi = (Bmi,1, Bmi,2,..., Bmi,D) for a typical problem with the number of dimensions D (*d= 1:D*), which randomly generates between the minimum BMmin = (Bmmin,1, Bmmin,2,..., Bmmin,D) and maximum BMmax = (Bmmax,1, Bmmax,2, . . . , Bmmax,D) values of the problem parameters range as follows:

$$BM_i = BM_{\min} + rand(1,D) \times (BM_{\max} - BM_{\min}); i = 1 : N_{pop}\infty \tag{2.1}$$

The movement of the BMi blood mass within the veins is determined by the applied force or pressure. The mass always goes in the direction where conditions are more favorable. As a result, its objective function (amount of force or pressure) has a lower value.

The occurrence of blocked arteries in the heart can be modeled as a situation where locally optimal solutions become trapped. In the real world, it is desirable to avoid such scenarios. The optimization process of the program will continue as long as the body is functioning. Based on the positions of the particles and the values of their objective functions, the circulatory cycle phase is then modeled.

$$BM_i^{new} = BM_i + K_{i1} \times P_i \times \left(BM_i - BM_1\right) + K_{23} \times P_i \times \left(BM_3 - BM_2\right) \tag{2.2}$$

$$\begin{cases} 1; F\left(BM_i\right) \langle F\left(BM_j\right) \\ -1; F\left(BM_i\right) \rangle F\left(BM_j\right) \\ 0; F\left(BM_i\right) = F\left(BM_j\right) \end{cases} \tag{2.3}$$

The parameter Kij determines the flow of the ith blood mass (BMi) through the arteries. Pi is a value ranging from 0 to 1, which depends on the size of the problem. In each circulation cycle, the algorithm calculates the displacement of the blood mass and works towards achieving a better value.

Deoxygenated blood, or the weaker population in optimization, is dealt with by the pulmonary circulation, as was previously described. In actuality, at each repetition the population is sorted in the CSBO, and the NR numbers of the weakest population are sent to the lungs to take up oxygen.

$$BM_i^{new} = BM_i + \left(\frac{randn}{it}\right) \times randc\left(1, D\right), i = 1 : NR \tag{2.4}$$

In (2.1), randc stands for the random vector from the Cauchy probability distribution, randn stands for the random normal number, it signifies the current algorithm iteration, and D stands for the dimension of the optimization problem. For this group, the pulmonary circulation also affects the pi in the following ways:

$$P_i = rand\left(1, D\right), i = 1 : NR \tag{2.5}$$

The weakest sorted population's NR numbers, as previously mentioned, are directed to the pulmonary circulation. To circulate through the body, the remaining population (NL = Npop - NR) with better fitting values enter the systemic circulation with a renewed quantity, as represented in the following model:

$$BM_{i,j}^{new} = BM_{i,j} + P_i * \left(BM_{3,j} - BM_{2,j} \right) \tag{2.6}$$

The systemic circulation also corrects the value of pi for this group of population in the following manner:

$$P_i = \frac{F\left(BM_i\right) - F_{worst}}{F_{Best} - F_{worst}}, i = 1 : NL \tag{2.7}$$

Where FWorst represents the worst result and FBest represents the best result achieved by the cost function up to the current iteration.

The optimization cycle continues for the specified number of iterations. During each iteration, every member of the population evaluates their new position and accepts it if it yields a better value for the fitness function, similar to other metaheuristic algorithms.

2.4.Common Metaheuristic Algorithms used in solving OPF problems

2.4.1.Moth-flame optimization algorithm [25]

The MFO algorithm is a new metaheuristic inspired by the nocturnal navigation mechanism used by butterflies in nature. This distinctive mechanism is mathematically modeled in MFO to perform global optimization tasks. In MFO, the search agents are represented by a population of night butterflies, each with a specific position in a given solution space. Additionally, the MFO approach also considers a set of NF flames (or artificial lights) randomly distributed around this solution space. Each flame also has a specific position, similar to how butterflies are "attracted" to nearby light sources. It is assumed that each butterfly "i" spirals towards a given flame "j". In this sense, while the positions of butterflies and flames represent solutions, only butterflies are true search agents, whereas flames represent the best NF solutions found so far by the MFO search process.

Taking this into consideration, at each iteration "k", each butterfly is first assigned to a particular flame, and then a movement operator, modeled using a logarithmic spiral, is applied to update the position of each agent.

Figure 2-5 shows the transverse orientation demonstrated by moths during navigation

Figure 2-6 shows (a) butterfly flying around a light source; and (b) path of navigation around the light source

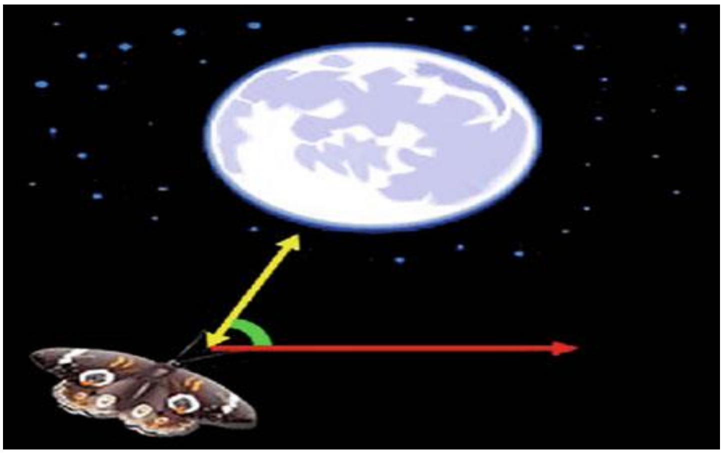

Figure 2-5 : Transverse Orientation Demonstrated by Moths During Navigation

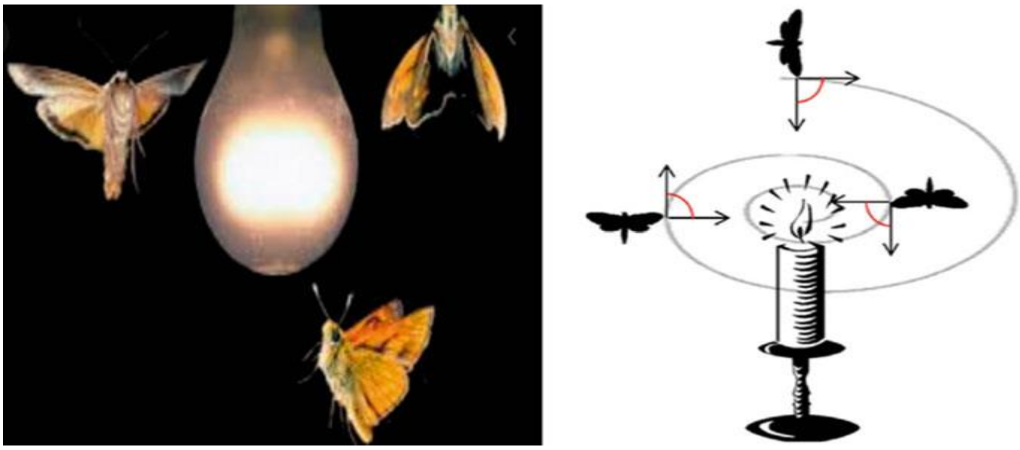

Figure 2-6 :(a) Butterfly Flying around a Light Source; (b) Path of Navigation around the Light Source

2.4.2. Particle Swarm Optimization (PSO) [27]

Particle Swarm Optimization (PSO) is a parallel optimization technique developed by Kennedy and Eberhart as an alternative to traditional genetic algorithms. They are inspired by the coordinated movements of flocks of birds insect swarms (or schools of fish or insect swarms). Similar to how these animals move in groups to find food sources or avoid predators, particle swarm algorithms search for solutions to optimization problems.

In this algorithm, individuals are called particles, and the population is referred to as a swarm. Each particle decides its next movement based on its own experience, which is represented by the best position it has encountered so far, and the experience of its best neighbor. The neighborhood can be defined spatially, for example, by considering the Euclidean distance between the positions of two particles, or socially (position in the swarm). The particle's new velocity and direction are determined by three tendencies: a propensity to follow its own path, a tendency to move back to its best position, and a tendency to move towards its best neighbor.

Particle swarm algorithms can be applied to both discrete and continuous data. They have been tested and proven efficient for various knowledge extraction tasks.

Figure 2-7 shows the concept of changing a research point using PSO

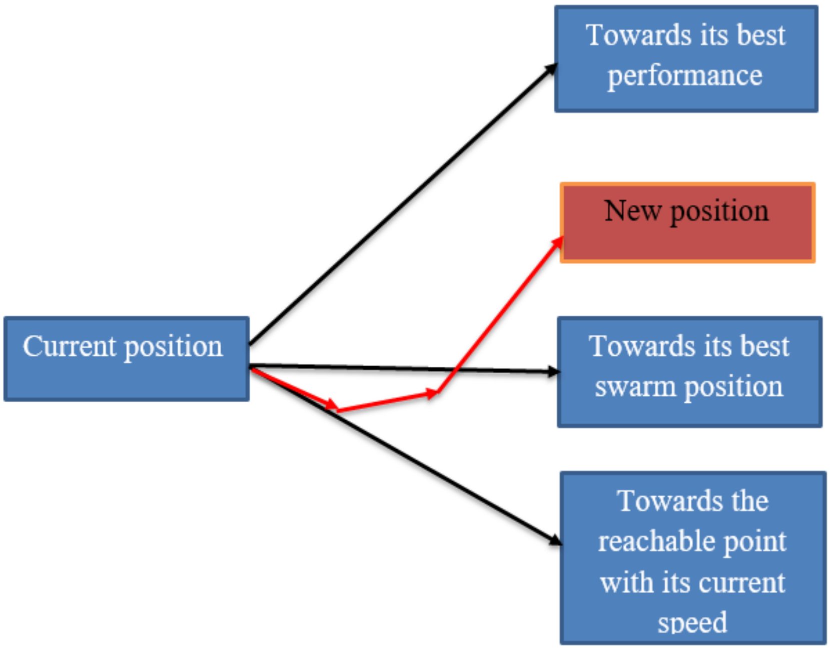

Figure 2-7 : Concept of changing a research point using PSO [28]

2.4.3.Black Widow Optimization Algorithm (BWOA) [29]

This method of optimization is inspired by the hunting behavior of black widow spiders. The algorithm aims to search for and gradually improve solutions by using exploration and exploitation mechanisms.

The proposed algorithm follows a flow diagram. Like other evolutionary algorithms, it starts with an initial population of spiders, where each spider represents a potential solution. These initial spiders attempt to reproduce in pairs to generate a new generation.

They begin mating to produce a new generation in parallel. Just like in nature, each pair mates in its own web, separate from the others. In the real world, around 1000 eggs are produced in each mating, but eventually, only a few baby spiders survive - the stronger ones. In this algorithm, to reproduce, a table called "alpha" must also be created, with the same length as the widow table, containing random numbers. Then, offspring is produced using α according to the following equation (equation 1), where $x1$ and $x2$ are the parents, and $y1$ and $y2$ are the offspring.

$$\begin{cases} Y_1 = a * x_1 + (1-a) * x_2 \\ y_2 = a * x_2 + (1-a) * x_1 \end{cases} \quad (2.8)$$

This process is repeated N_VAR/2 times, where N_VAR represents the number of variables in the problem, to ensure that randomly selected numbers do not repeat. Finally, the offspring and the mother are added to an array and sorted based on their fitness value. Then, according to the cannibalism rate, some of the best individuals are added to the newly generated population.

Figure 2-8 shows female black widow (a) in her web with egg sac, and (b) on her web

Figure 2-8 : (a) Female black widow in her web with egg sac**.** (b) Female black widow on her web.

2.5.Conclusion

In this chapter, we have presented a detailed explanation of metaheuristic optimization methods. This has allowed us to gain a better understanding of the concepts and principles used by metaheuristic algorithms and their potential applications. We introduced the Circulatory System Based Optimization (CSBO) algorithm, analyzing its unique features. Additionally, we briefly discussed the study of other algorithms, such as Moth Flame Optimization (MFO), Particle Swarm Optimization (PSO), and the Black Widow Optimization Algorithm (BWOA). This chapter provides an introduction and a comprehensive overview of metaheuristic techniques and their diverse approaches to solving complex optimization problems. The following chapter presents the simulation results of our work, clearly explaining the algorithmic process of these methods and their application in power flow optimization with the integration of renewable energy sources.

Chapter 3: Solution of (OPF) Problems in Modern Power Systems

Chapter 3:

SOLUTION OF (OPF) PROBLEMS IN MODERN POWER SYSTEM

3.1.Introduction

Renewable energy sources (RES) like solar, wind, and hydro have become increasingly popular for use in stochastic power system operations. However, they require the ability to make optimal decisions in uncertain conditions. It is crucial to determine the best operating parameters for the electric grid and schedule various energy sources efficiently.

To deal with the stochastic nature of (RES) we have suggested the implementation of a new meta-heuristic algorithm called circulatory system-based optimization (CSBO) in solving the OPF problem while taking into consideration the integration of RES (solar, wind, and small-hydro power) and their stochastic nature. The structure of the chapter is as follows: The OPF study with stochastic wind, solar, and hydropower problem formulation is described in Section 2. In Section 3, we have presented a detailed discussion concerning the treated cases and the obtained results.

3.2.Solving OPF problems with stochastic PV, Wind and hybrid PV-small-hydro generators

In traditional electric grids, the optimal power flow analysis is primarily focused on conventional power generators fueled by fossil fuels. However, as electricity markets have been liberalized and renewable energy sources have been integrated, the study of OPF has become more complex, leading to a significant increase in the complexity of the objective function. This complexity arises from the diverse functions that consider the variability and uncertainty inherent in the problem formulation.

The primary objective of incorporating RES generators into the grids is to minimize transmission line losses and enhance the reliability and quality of electric grids. Moreover, they contribute to reducing environmental pollution. Additionally, as the injected power from RES continues to increase, it becomes crucial to determine the optimal contribution of each generator in the system. Therefore, efficient energy management and optimal scheduling of different resources can effectively support the diverse missions of electric power system operators, ultimately reducing the overall cost of electricity generation. [30]

3.2.1.Optimal power flow model

The important goal of solving OPF problems is to determine the optimal values of control variables so that they minimizing a certain objective function while respecting all the physical and security constraints. Mathematically, the OPF problem is expressed using the following equation

$$Minimize\, F(x,u) \tag{3.1}$$

$$subject\ to: \begin{cases} g(x,u)=0 \\ h(x,u)\le 0 \end{cases} \tag{3.2}$$

Where: $F(x,u)$ presents the objective function, x and u are the vectors of control and state variables, respectively, $g(x,u)$ and $h(x,u)$ are the equality and inequality constraints, respectively.

3.2.1.1.Objective Functions

In this study, three objective functions are proposed, minimization of total generation cost, total active power loss, and cost with emission effect.
The generation cost of thermal generators considering the valve point effect is given as follows:

$$C_{\mathrm{T}}\left(P_{TG}\right)=\sum_{i=1}^{N_{TG}} a_i + b_i P_{TGi} + c_i P_{TGi}^2 + \left| d_i \times \sin\left(e_i \left(P_{TGi}^{\min} - P_{TG} \right)\right)\right| \tag{3.3}$$

Where a_i , b_i , c_i , d_i and e_i represent the cost coefficients related to i-th thermal generator P_{TGi} , $P_{TGi}^{\min}$ is the minimum value of power corresponding to i-th thermal generator. N_{TG} is the number of thermal generators;

- **Case 1:** the first objective of OPF is the minimization of total generation cost considering both thermal generators and RESs can be formulated as:

$$\begin{aligned} F_{Obj}^{1} = {} & C_T\left(P_{TG}\right)+\left[C_{W,j}\left(P_{WGs,j}\right)+C_{RW,j}\left(P_{WG,j}-P_{WAv,j}\right)+C_{PW,j}\left(P_{WAv,j}-P_{WG,j}\right)\right] \\ & +\left[C_{S,k}\left(P_{SG,k}\right)+C_{RS,k}\left(P_{SG,k}-P_{SAv,k}\right)+C_{PS,k}\left(P_{SAv,k}-P_{SG,k}\right)\right]+\left[C_{SHG}(P_{SHG})+C_{RSH}(P_{SHG}-P_{SHAv})+C_{PSH}(P_{SHAv}-P_{SHG})\right] \end{aligned} \tag{3.4}$$

- **Case 2:** the second objective of OPF is the minimization of total active power loss in the electric grid, which can be formulated as:

$$F_{Obj}^{2} = \text{minimize } P_{Losses} = \sum_{q=1}^{nl} G_{q(ij)}\left[V_i^2 + V_j^2 - 2\, V_i V_j \cos\,(\delta_i - \delta_j)\right] \tag{3.5}$$

where nl is the total number of transmission lines, $G_{q(ij)}$ is the conductance of the branch i-j, V_i and V_j are the voltages at bus i and j respectively, $\delta_{ij} = \delta_i - \delta_j$, is the difference in voltage angles between them.

- **Case 3:** the final objective of OPF is to minimize both generation cost and emission by including the carbon tax as penalty, which can be formulated as:

$$F_{Obj}^3 = F_{Obj}^1 + C_{tax} \times E \tag{3.6}$$

$$E = \sum_{i=1}^{N_{TG}} \left[\left(\alpha_i + \beta_i P_{TGi} + \gamma_i P_{TGi}^2 \right) + \delta_i \exp\left(\varepsilon_i P_{TGi} \right) \right] \tag{3.7}$$

3.2.1.2. System Constraints

While solving OPF objectives, different equality and inequality constraints are to be respected. These constraints are expressed as follow:

Equality constraints

$$\begin{cases} P_{Gi} - P_{di} - V_i \sum_{j=1}^{NB} V_j \left[G_{ij} \cos(\delta_{ij}) + B_{ij} \sin(\delta_{ij}) \right] = 0 \\ Q_{Gi} - Q_{di} - V_i \sum_{j=1}^{NB} V_j \left[G_{ij} \sin(\delta_{ij}) - B_{ij} \cos(\delta_{ij}) \right] = 0 \end{cases} \tag{3.8}$$

where P_{Gi}, Q_{Gi} are the active and reactive power of generation, P_{di}, Q_{di} are the active and reactive power of demand and NB is the total number of bus of the power system.

Inequality constraints

- **Generator constraints**

$$P_{TGi}^{\min} \le P_{TGi} \le P_{TGi}^{\max} \qquad i = 1, 2.....N_{TG} \tag{3.9}$$

$$P_{WG}^{\min} \le P_{WG} \le P_{WG}^{\max} \tag{3.10}$$

$$P_{SG}^{\min} \le P_{SG} \le P_{SG}^{\max} \tag{3.11}$$

$$P_{SHG}^{\min} \le P_{SHG} \le P_{SHG}^{\max} \tag{3.12}$$

$$Q_{TGi}^{\min} \le Q_{TGi} \le Q_{TGi}^{\max} \tag{3.13}$$

$$Q_{WG}^{\min} \le Q_{WG} \le Q_{WG}^{\max} \tag{3.14}$$

$$Q_{SG}^{\min} \le Q_{SG} \le Q_{SG}^{\max} \tag{3.15}$$

$$Q_{SHG}^{\min} \le Q_{SHG} \le Q_{SHG}^{\max} \tag{3.16}$$

- **Prohibited operating zones POZs**

$$P_{TG2}^{\min\, poz,j} \le POZ_{TG2}^{j} \le P_{TG2}^{\max\, poz,j} \tag{3.17}$$

- **Security constraints**

$$V_{Gi}^{\min} \le V_{Gi} \le V_{Gi}^{\max} \qquad i = 1, 2.....N_{TG} \tag{3.18}$$

$$V_{Li}^{\min} \le V_{Li} \le V_{Li}^{\max} \qquad i \in NL \tag{3.19}$$

$$S_i \le S_i^{\max} \qquad i \in NTL \tag{3.20}$$

3.2.2. Modeling the uncertainty of renewable energy generators

Due to stochastic nature of RES, it is required to present the model uncertainty adopted in this study in terms of operation and planning of power systems. The wind speed is a random variable, wind uncertainty is modeled using the Probability Density Function (PDF) is to obtain its distribution employing shape factor (k) and scale factor (c). Mathematically can be written as: [29]

$$f_\upsilon(S) = \left(\frac{k}{c}\right)\left(\frac{S}{c}\right)^{(k-1)} \times \exp - \left(\frac{S}{c}\right)^k \quad for \;\; 0 < S < \infty \tag{3.21}$$

The wind power model

The output wind-power according to wind speed, is expressed as:

$$P_w(\upsilon) = \begin{cases} 0, & \text{for } \;\; \nu \langle \nu_{in} \;\; and \;\; \nu \rangle \nu_{out} \\ P_{wr}\left(\dfrac{\nu - \nu_{in}}{\nu_r - \nu_{in}}\right) & \text{for } \;\; \nu_{in} \le \nu \le \nu_r \\ P_{wr} & \text{for } \;\; \nu_r \le \nu \le \nu_{out} \end{cases} \tag{3.22}$$

With ν_{in} defines the turbine cut-in, ν_r is the rated wind speed and ν_{out} pertains cut-out wind speed, and P_{wr} rated output-power. [31,32]

3.2.2.1.Wind power probability for different wind-speeds[31,32]

The equation (22) states that, when ν_{in} is more than ν and down than ν_{out}, the output of power equal to zero. But the wind turbine output the rated-power P_{wr} for the condition of $\nu_r \le \nu \le \nu_{out}$. To model this fact, the probabilities of wind power is modeled as:

$$f_w(P_w)\{P_w = 0\} = 1 - \exp\left[-\left(\frac{\nu_{in}}{\alpha}\right)^\beta\right] + \exp\left[-\left(\frac{\nu_{out}}{\alpha}\right)^\beta\right] \tag{3.23}$$

$$f_w(p_w)\{p_w = p_{wr}\} = 1 - \exp\left[-\left(\frac{\nu_r}{\alpha}\right)^\beta\right] + \exp\left[-\left(\frac{\nu_{out}}{\alpha}\right)^\beta\right] \tag{3.24}$$

Outside to the discrete zones, the output of wind power is remained continuous for the condition of $\nu_{in} \le \nu \le \nu_r$, This probability is modeled by the following equation:

$$f_w\left(p_w\right)=\frac{\beta\left(\nu_r-\nu_{in}\right)}{\alpha^{\beta}*P_{wr}}\left[\nu_{in}+\frac{P_w}{P_{wr}}\left(\nu_r-\nu_{in}\right)\right]^{\beta-1}\exp\left[-\left(\frac{\nu_{in}+\frac{P_w}{P_{wr}}\left(\nu_r-\nu_{in}\right)}{\alpha}\right)^{\beta}\right] \quad (3.25)$$

The solar-irradiance to energy conversion for the PV generator is modeled as follow:

$$P_s\left(G\right)=\begin{cases}P_{sr}\left(\frac{G^2}{G_{std}R_c}\right) & \text{for } 0\le G\le R_c\\ P_{sr}\left(\frac{G^2}{G_{std}}\right) & \text{for } G\ge R_c\end{cases} \quad (3.26)$$

3.2.3.Generation Cost minimization for renewable sources[5]

When integrating renewable sources into the power grid, certain conditions must be taken into account, including the uncertainty and intermittency of these sources. Typically, private entities own wind farms and solar PV systems, which enter into purchase agreements for scheduled power with the independent system operator (ISO). As a result, the cost of these power generators can be divided into several components, namely direct cost, reserve cost, and penalty cost. The direct cost of wind and solar PV generators is outlined below.

The direct cost associated with wind power from the j^{-th} plant is expressed as a function of the scheduled power. [33]

$$C_{W,j}\left(P_{WG,j}\right)=g_jP_{WG,j} \quad (3.27)$$

Like the wind power plant, the direct cost related to the k^{-th} solar PV plant is

$$C_{S,k}\left(P_{SG,k}\right)=h_kP_{SG,k} \quad (3.28)$$

Where g_j and h_k present the coefficient of direct cost corresponding to j^{th} wind generator and k^{th} solar generator respectively. $P_{WG,j}$ and $P_{SG,k}$ are the scheduled power from the appropriate generator. The direct cost function for the combination of solar photovoltaic and small hydro generation plant is given by [33]

$$C_{SHG}(P_{SHG})=C(P_{SG}+P_{HG})=g_{SG}P_{SG}+h_{HG}P_{HG} \quad (3.29)$$

Where P_{SHG} is the scheduled power from incorporated renewable resources, P_{SG} and P_{HG} present the electric power contribution from the solar and hydro generators, respectively. g_{SG} and h_{HG} are the coefficients of direct-cost corresponding to solar PV unit and small hydro unit, respectively.

Due to stochastic nature of renewable energy sources, there are two possibilities tendencies which is, overestimation and underestimation.

First case, when the actual power generated by renewable generators (PV, or combined PV and hydropower) less than the estimated-quantity in term of power, called overestimation. Second case is underestimation realised when estimated-quantity power is less than actual power.

3.2.3.1.The reserve cost caused with overestimation is presented as follows[5]:

$$\begin{aligned} C_{RW,j}\left(P_{WG,j}-P_{Av,j}\right) &= K_{RW,j}\left(P_{WG,j}-P_{WAv,j}\right) \\ &= K_{RW,j}\int_{0}^{P_{WG,j}}\left(p_{WG,j}-P_{W,j}\right)\ f_W\left(P_{W,j}\right)dp_{W,j} \end{aligned} \tag{3.30}$$

$$\begin{aligned} C_{RS,k}\left(P_{SG,k}-P_{SAv,k}\right) &= K_{RS,k}\left(P_{SG,k}-P_{SAv,k}\right) \\ &= K_{RS,k} * f_S\left(P_{SAv,k}<P_{SG,k}\right) * \left[P_{SG,k}-E\left(P_{SAv,k}<P_{SG,k}\right)\right] \end{aligned} \tag{3.31}$$

$$\begin{aligned} C_{RSH}(P_{SHG}-P_{SHAv}) &= K_{RSH}(P_{SHG}-P_{SHAv}) \\ &= K_{RSH} * f_{SH}(P_{SHAv}<P_{SHG}) * \left[P_{SHG}-E(P_{SHAv}<P_{SHG})\right] \end{aligned} \tag{3.32}$$

Where $K_{RW,j}$ is the reserve cost coefficient corresponding to j^{th} wind generation unit, $P_{WAv,j}$ is the actual power delivered by the same unit, $f_W\left(p_{W,j}\right)$ is the PDF of wind power corresponding to j^{th} wind power plant. $K_{RS,k}$ is the reserve cost coefficient corresponding to k^{th} solar power unit, $P_{SAv,k}$ is the actual power delivered by the same unit, $f_S\left(P_{SAv,k}<P_{SG,k}\right)$ is the probability of solar energy curtailment from the scheduled power ($P_{SG,k}$) and $E\left(P_{SAv,k}>P_{SG,k}\right)$ is the prediction of solar-power above $P_{SG,k}$. K_{RSH} is the coefficient of reserve cost corresponding to the combined system, P_{SHAv} is the actual power delivered by the same plant, $f_{SH}(P_{SHAv}<P_{SHG})$ is the probability of combined system energy curtailment from the scheduled power P_{SHG} and $E(P_{SHAv}<P_{SHG})$ is the prediction of delivered power below P_{SHG} .

3.2.3.2.The underestimation of power is related to the penalty terms which defined by second case. Mathematically, can be expressed as follows[5]:

$$C_{PW,j}\left(P_{WAv,j}-P_{WG,j}\right)=K_{PW,j}\left(P_{WAv,j}-P_{WG,j}\right)=K_{PW,j}\int_{P_{WG,j}}^{P_{Wr,j}}\left(p_{W,j}-p_{WG,j}\right)f_W\left(P_{W,j}\right)dp_{W,j} \tag{3.33}$$

$$C_{PS,k}\left(P_{SA,k}-P_{SG,k}\right)=K_{PS,k}\left(P_{SAv,k}-P_{SG,k}\right)=K_{PS,k}*f_S\left(P_{SAv,k}>P_{SG,k}\right)*\left[E\left(P_{SAv,k}>P_{SG,k}\right)-P_{SG,k}\right] \quad (3.34)$$

$$C_{PSH}(P_{SHAv}-P_{SHG})=K_{PSH}(P_{SHAv}-P_{SHG})=K_{PSH}*f_{SH}(P_{SHAv}>P_{SHG})*[E(P_{SHAv}>P_{SHG})-P_{SHG})] \quad (3.35)$$

Where $K_{PW,j}$ is the coefficient of penalty cost relate to j-th wind power generator, $P_{Wr,j}$ is the rated output power from the plant, $K_{PS,k}$ is the penalty cost coefficient corresponding to k^th solar power generator, $f_S\left(P_{SAv,k}>P_{SG,k}\right)$ is the probability of solar energy surplus of the scheduled power $P_{SG,k}$ and $E\left(P_{SAv,k}>P_{SG,k}\right)$ is the prediction of solar-power above $P_{SG,k}$. K_{PSH} is the coefficient of penalty cost corresponding to the combined system, $f_{SH}(P_{SHAv}>P_{SHG})$ is the probability of combined system energy surplus of the scheduled power P_{SHG} and $E(P_{SHAv}>P_{SHG})$ is the prediction of the combined system power above P_{SHG}.

3.2.4. The proposed optimization algorithm

Generate initial blood mass $\boldsymbol{BM_i}$using Equation (2.1)
Calculate $\boldsymbol{p_i}$ using Equation (2.5) and (2.7)
it ← 0
FE ← $\boldsymbol{N_{pop}}$
While FE ≤ $\boldsymbol{N_{pop}}$
it ← it + 1
For i = 1 : $\boldsymbol{N_{pop}}$
Calculate $\boldsymbol{K_{i1}}$ and using $\boldsymbol{K_{23}}$Equation (2.3)
Generate a new blood masse $\boldsymbol{BM_i^{new}}$using Equation (2.2)
Update the new position of blood mass i
FE ←FE + 1
end
for i = 1 :NR
for j = 1 : D
if rand > 0,9
perform the pulmonary circulation using Equations (2.4)
else
$\boldsymbol{BM_{i\,j}^{new}} = \boldsymbol{BM_{i\,j}}$
end
End
FE← FE + 1
Calculate $\boldsymbol{p_i}$for the weakest population using Equations (2.5)
end
for i = 1 :NL
Perform the systematic circulations using Equations (2.6)
Update the new position of blood mass i
Calculate $\boldsymbol{p_i}$ using Equation (2.7)
FE ← FE + 1
end
Update the best solution
end
Return the best solution

3.2.5. Numerical results and analysis

In the first part, three scenarios were considered on the modified IEEE 30-bus test system by MATLAB. The modification is to insert wind generator, solar generator and combined solar PV and small hydropower at bus #5, #11 and #13, respectively.

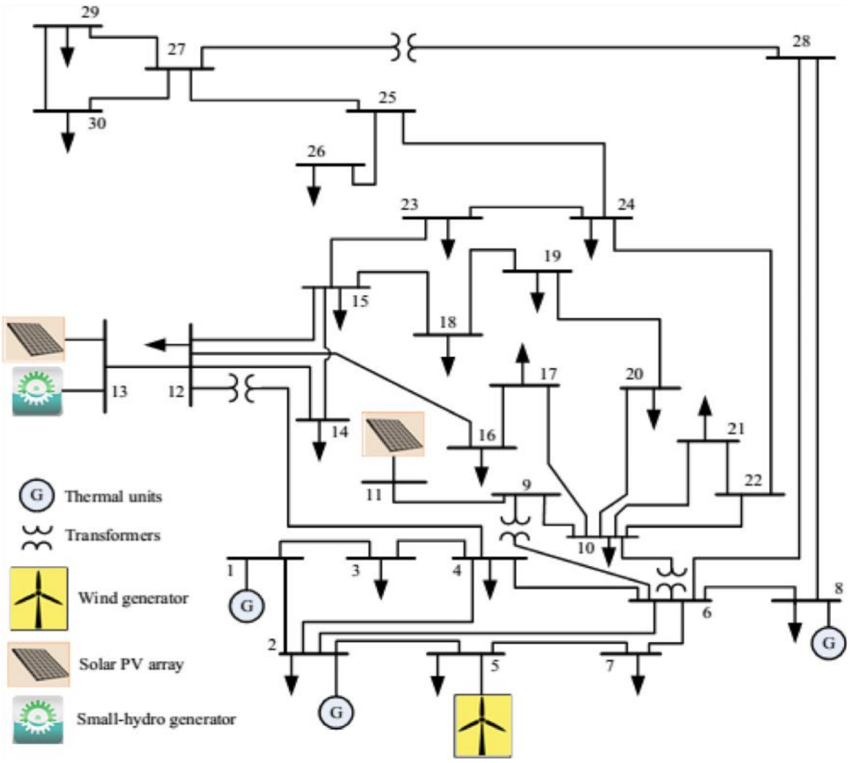

Figure 3-1 : Modified IEEE 30 bus system [5]

Table 3-1 indicates the characteristics of the modified IEEE 30-bus test systems.

- In scenario I, total generation cost is minimized.
- In second scenario II, total active power loss minimization is considered.
- In the last one, both of generation cost and pollution were minimized while respecting all imposed constraints.

The proposed CSBO is executed to solve the three cases, and some other algorithms are chosen to compare with CSBO to further indicate its performance and consistency to find a near-optimal feasible solution. Tables 3-2 – 3-3 present the coefficients of thermal generators and limitations of both soft and hard- variables.

Table 3.1 : Characteristics of the modified test systems

Elements	**IEEE 30-bus**
no. of buses	30
no. of transmission lines	41
no. of generators	06
no. of thermal generators	03
Number of renewable generators	03
no. of load buses	24
no. of control variables	12
Initial Real and reactive power demand	283.4 MW ; 126.2 Mvar

Table 3.2: Thermal generators cost and emission coefficients for test system

Generator	Bus	a	b	c	d	e	α	β	γ	δ	ε
TG1	1	0	2	0.0038	18	0.037	0.04091	-0.05554	0.06490	0.0002	6.667
TG2	2	0	1.75	0.0175	16	0.038	0.02543	-0.06047	0.05638	0.0005	3.333
TG3	8	0	3.25	0.0083	12	0.045	0.05326	-0.03550	0.03380	0.0020	2.000

Table 3.3 : Upper and lower bounds of control and state variables for test system I

	Control variables							**State variables**					
Variables	P_{TG1}	P_{TG2}	P_{TG3}	P_{WG}	P_{SG}	P_{SHG}	V_{gi}	Q_{TG1}	Q_{TG2}	Q_{TG3}	Q_{WG}	Q_{SG}	Q_{SHG}
Min	50	20	10	0	0	0	0.95	-20	-20	-15	-30	-25	-20
Max	140	80	35	75	60	50	1.1	150	60	40	35	30	25

Case 1: total generation cost minimization

In the first case, the primary goal is to minimize the total generation cost considering wind, solar and combined solar and small hydro generators. Obtained results are based on the Weibull, lognormal and Gumbel PDF parameters. Table 3-4 indicates PDF parameters of renewable energy sources that have been presented in [5]. Weibull fitting and wind speed frequency distributions are presented in Figure 3-2 reached from the simulation of 8000 Monte Carlo scenarios Figure 3-3 presents the lognormal fitting and solar irradiance frequency distributions obtained from the simulation of 8000 sample size of Monte Carlo. Figure 3-4 presents active power distribution of solar PV generator at bus 11.

In this study, combined solar PV with small hydro generator is used in place of thermal generator at bus 13. Figure 3-5 indicates the lognormal fitting and solar irradiance accessible of solar PV generator at the same bus. while Figure 3-6 indicates Gumbel fitting and river flow rate frequency distribution from small hydro generator. Like last time, diagrams are generated after the simulation of 8000 Monte Carlo scenarios. The capacity of solar PV generator is 45 MW while for small hydropower is 5 MW. Figure 3-7 and Figure 3-8 present the histograms of both available solar power and hydropower for the site and from the solar PV generator and small hydro generator respectively at bus 13. Table 3-5 indicates direct, penalty and reserve cost coefficients of renewable energy sources.

Table 3.4 : PDF parameters of renewable energy sources

Wind-power generating unit		
No of turbines	Rated power, P_{wr} (MW)	Weibull PDF parameters
25	75	l=9 ; p=2
Photovoltaic power plant		
Rated power, $\boldsymbol{P_{sr}}$ (MW)	Lognormal PDF parameters	
50	μ=5.2 σ=0.6	
Combined solar and small hydro-power		
Photovoltaic rated power $\boldsymbol{P_{sr}}$(MW)	Lognormal PDF parameters	
45	μ=5.0 σ=0.6	
Small hydro rated power $\boldsymbol{P_{hr}}$(MW)	Gumbel PDF parameters	
5	λ=15 γ=1.2	

Table 3.5: The different cost coefficients of renewable energy sources

Direct cost coefficient			**Penalty cost coefficient**			**Reserve cost coefficient**		
Wind	Solar	Small hydro	Wind	Solar	Small hydro	Wind	Solar	Small hydro
$g_j = 1.7$	$h_k = 1.6$	$h_{HG} = 1.5$	$K_{PW,j} = 1.4$	$K_{PS,k} = 1.4$	$K_{PSH} = 1.4$	$K_{RW,j} = 3$	$K_{RS,k} = 3$	$K_{RSH} = 3$

The figure 3-2 represent the Wind speed distribution at bus 5.

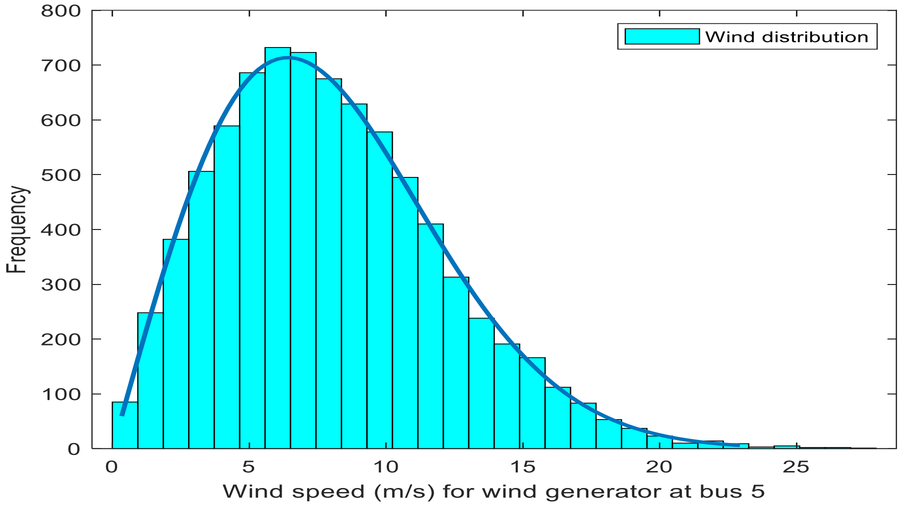

Figure 3-2 : Wind speed distribution at bus 5

The figure 3-3 represent the Solar irradiance for PV generator at bus 11

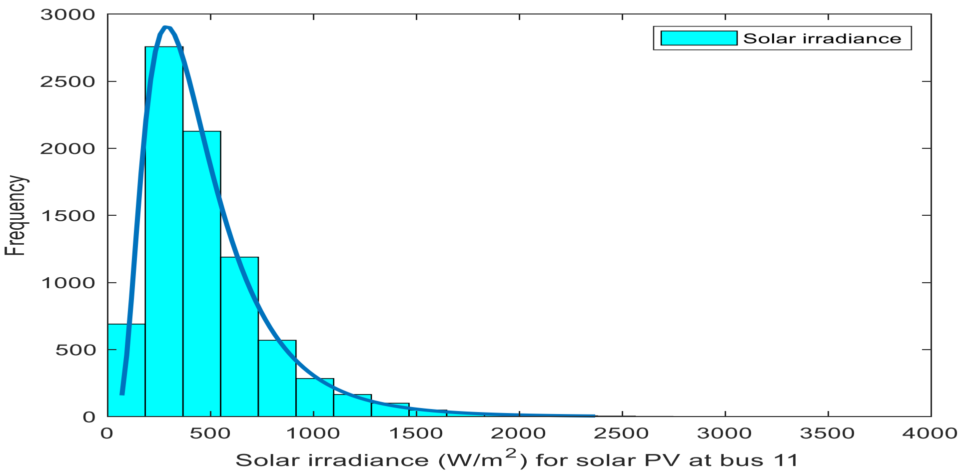

Figure 3-3 **:** Solar irradiance for PV generator at bus 11

The figure 3-4 represent the Active power distribution of solar PV generator at bus 11

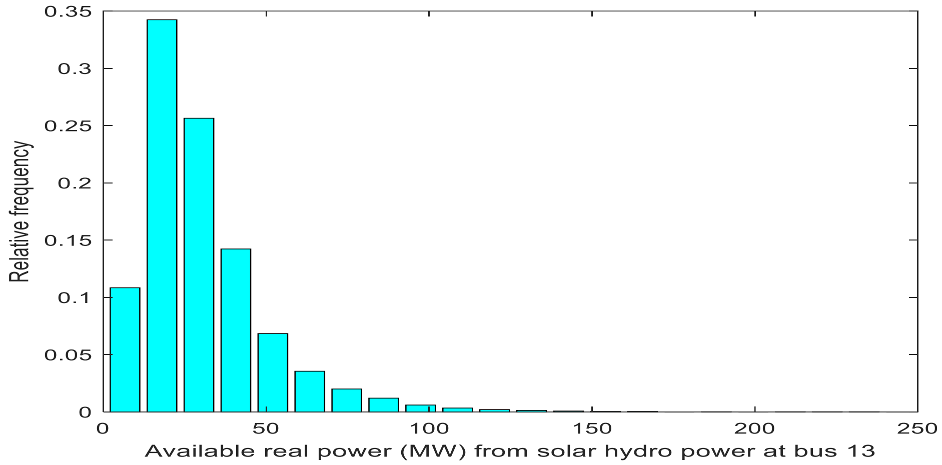

Figure 3-4: Active power distribution of solar PV generator at bus 11

The figure 3-5 represent the Solar irradiance for solar PV generator at bus 13

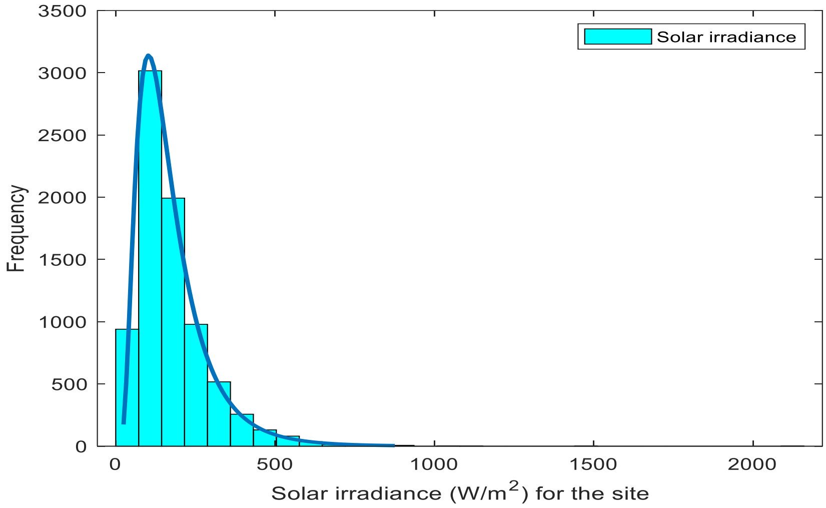

Figure 3-5 : Solar irradiance for solar PV generator at bus 13

The figure 3-6 represent the river flow rate for small hydro generator at bus 13

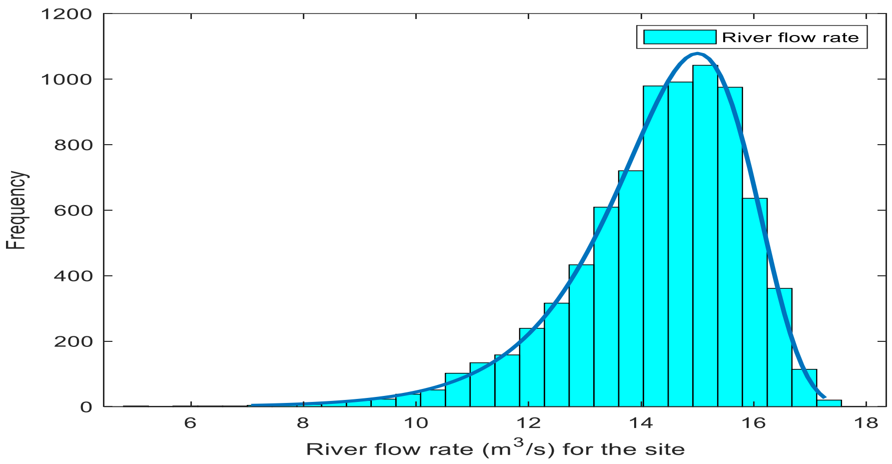

Figure 3-6 : River flow rate for small hydro generator at bus 13

The figure 3-7 represent the available solar power for the site and from the solar PV generator at bus 13.

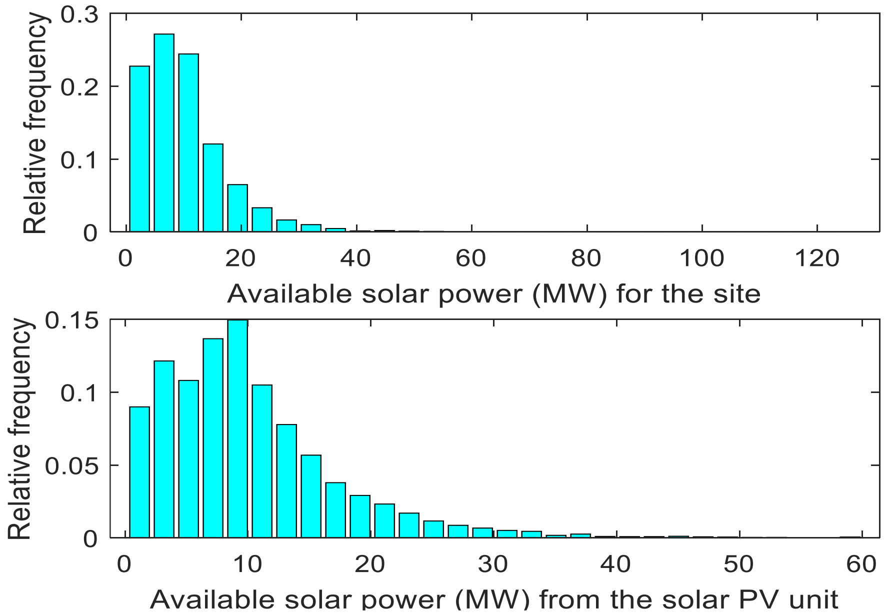

Figure 3-7: Available solar power for the site and from the solar PV generator at bus 13.

The figure 3-8 represent the Available hydropower for the site and from the small hydro generator at bus 13

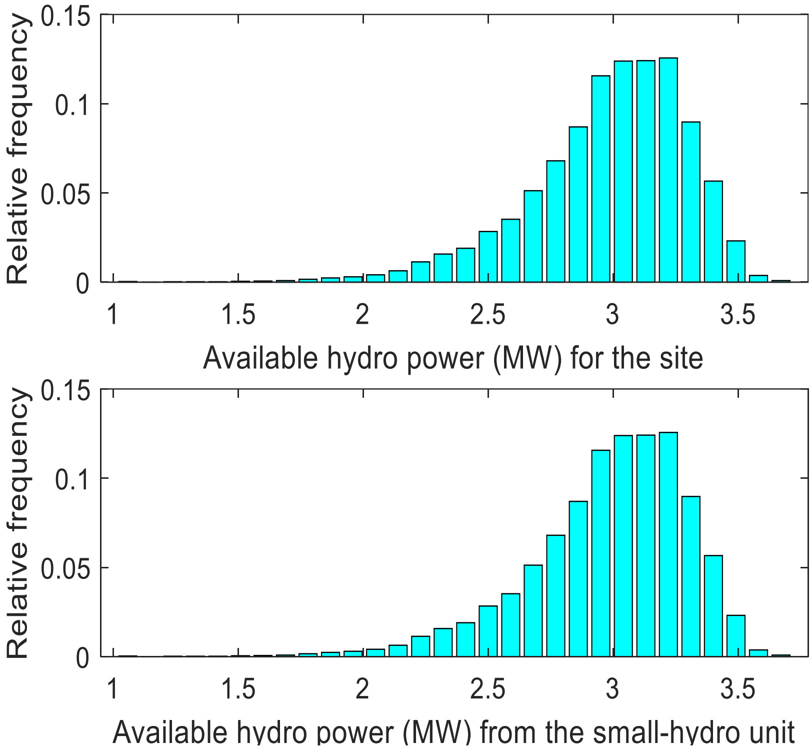

Figure 3-8 : Available hydropower for the site and from the small hydro generator at bus 13

Table 3.6 optimal results for the objective function and optimal control/state variables related to case 1 that were obtained by various algorithms, including CSBO, AEO, and GTO. These optimal values were within the permissible range specified in Table 3-3.

Table 3.7 compares the statistical results based on the minimum, average, maximum and standard deviation of the total generation cost obtained by CSBO with the chosen algorithms: BWOA, PSO, GSA, MFO, HS, and BMO given in ref. [5] as well as with implemented GTO and AEO. Through this comparison, it is clear that CSBO outperformed the rest of the algorithms in all statistical results within 30 independent runs of simulation. The minimum value of total generation cost obtained by CSBO is 787.3598 $/h. The proposed algorithm exceeds all optimization techniques, BWOA (791.4748), PSO (789.4849$/h), GSA (790.3496 $/h), MFO (789.5271$/h), HS (800.5362$/h), BMO (789.1248 $/h), GTO (789.2231$/h) and AEO (789.3185 $/h). The difference between the value obtained by CSBO and the worst value obtained by HS is 13.1764 $/h which is very important around 316.2336 $ cost saving per day and 115425.264 $ cost saving per year.

Table 3.6 : Optimal results obtained of case 1 for different algorithms

Variable	MFO[5]	BMO[5]	GTO	AEO	INFO	HS[8]	GSA[5]	PSO[5]	BWOA[5]	CSBO
P_{TG1}	134.90	134.91	134.91	134.91	134.93	134.9079	134.7760	134.9079	134.9088	135.23
P_{TG2}	40.004	40.000	42.58	40.45	41.99	65.0000	45.2135	40.0000	41.6666	39.62
P_{WG}	46.202	46.937	48.18	47.55	48.20	36.6795	47.1036	46.4294	45.4876	46.80
P_{TG3}	10.000	10.000	10.00	10.01	10.01	10.0000	10.8455	10.0000	11.8272	10.05
P_{SG}	44.727	43.799	39.66	41.54	40.09	31.8026	38.4926	44.7704	41.8719	40.66
P_{SHG}	13.304	13.483	13.97	14.79	14.06	11.6731	12.8524	13.0326	13.8799	16.85
V_1	1.0831	1.0835	1.077	1.076	1.075	1.0843	1.0816	1.0835	1.0520	1.086
V_2	1.0686	1.0691	1.064	1.060	1.061	1.0704	1.0678	1.0689	1.0429	1.068
V_5	1.0463	1.0476	1.039	1.037	1.041	1.0447	1.0450	1.0467	1.0351	1.041
V_8	1.0488	1.0493	1.040	1.041	1.041	1.0472	1.0471	1.0489	1.0367	1.045
V_{11}	1.1000	1.1000	1.098	1.100	1.099	1.1000	1.1000	1.1000	1.0380	1.096
V_{13}	1.0530	1.0524	1.052	1.067	1.061	1.0567	1.0535	1.0527	1.0380	1.053
Q_{TG1}	-	-0.7352	1.35	4.88	0.35	-0.2154	-1.4807	-0.2965	-15.403	12.53
Q_{TG2}	14.467	14.582	25.81	15.88	19.74	14.8635	15.5110	14.6635	10.9783	17.56
Q_{WG}	23.250	23.729	24.11	24.79	27.66	24.4993	22.7903	23.2576	35.6096	22.35
Q_{TG3}	37.050	37.064	38.38	38.83	38.84	36.4881	36.8058	36.8604	56.3782	39.53
Q_{SG}	28.608	28.425	30.00	29.96	29.80	27.7191	28.486	28.578	13.712	28.14
Q_{SHG}	14.885	14.477	17.04	22.46	20.30	16.3498	15.469	14.722	18.992	15.89
F_{Cost}	789.52	789.12	789.223	789.318	788.9417	800.5362	790.3496	789.4849	791.4748	787.3598

Table 3.7 : Comparison of statistical results of case 1 for different algorithms

Algorithms	Minimum	Maximum	Average	Std
INFO	788.94	790.61	789.73	4.46E-01
AEO	789.32	791.27	790.11	5.76E-01
GTO	789.22	791.48	790.13	5.90E-01
HS [5]	800.54	802.25	801.83	1.49E-01
BMO [5]	789.12	793.09	790.44	1.04E+00
MFO [5]	789.53	793.94	790.89	1.32E+00
GSA [5]	790.35	802.44	794.17	3.19E+00
PSO [5]	789.48	799.67	793.78	3.57E+00
BWOA [5]	791.47	796.53	793.70	1.20E+00
CSBO	**787.36**	**788.05**	**787.75**	**1.19E-0.1**

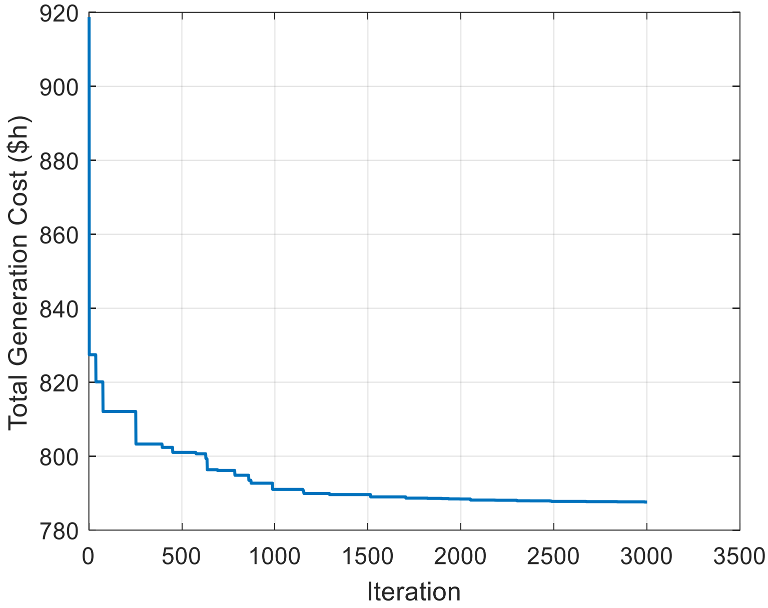

Figure 3-9: Convergence curve for OF in case 1

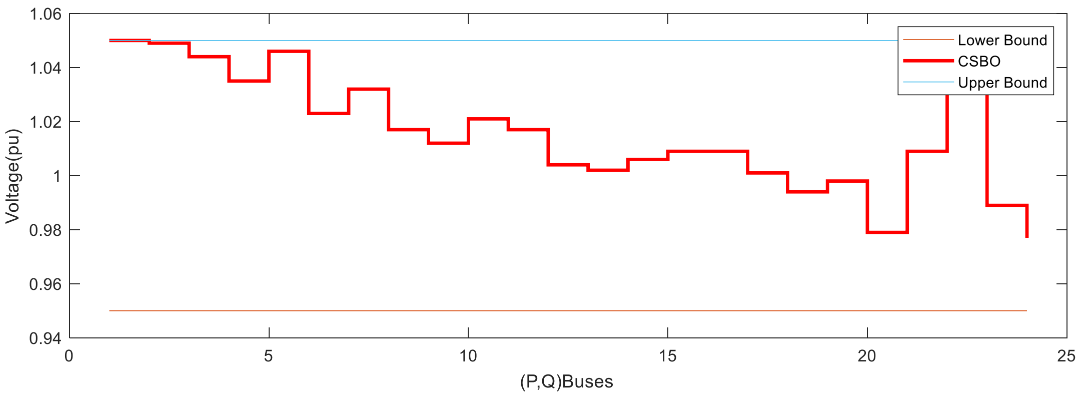

Figure 3-10. Voltage profiles in PQ buses of CSBO algorithm for case 1

Figure 3-9 represents the Convergence curve for OF in case 1, whereas figure3-10 represents Voltage profiles in PQ buses CSBO algorithm for case 1 as it can be seen the CSBO algorithm effectively maintains voltage profiles in PQ buses. The results clearly demonstrate the algorithm's capability ensuring that the voltage constraints are respected.

Case 2: Total Active Power Losses Minimization (TAPLM)

Table 3.8 presents the optimal results of the objective function, as well as the optimal values of the control and state variables for case 2, obtained using different algorithms. All the algorithms successfully satisfied all the constraints while achieving the optimal outcomes.

Table 3.9 displays the statistical results comparing CSBO with other algorithms in terms of minimizing total active power loss in the OPF problem. CSBO achieved a minimum power loss of 2.1059 MW, surpassing other optimization techniques except for INFO that achieved 2.09 MW. AEO

(2.1244 MW), BMO (2.1669 MW), MFO (2.1669 MW), PSO (2.1868 MW), BWOA (2.1876 MW), GTO (2.2212 MW), HS (2.5114 MW) and GSA (2.8962 MW). Figure 3.9 illustrates the convergence curve of the total active power loss.

Table 3.8: Optimal results obtained of case 2 for different algorithms

Variable	INFO	MFO[5]	HS[5]	BMO[5]	GTO	AEO	BWOA[5]	GSA[5]	PSO[5]	CSBO
P_{TG1}	50.01	50.0000	50.0013	50.0000	50.00	50.02	50.0000	53.9396	50.0000	50.07
P_{TG2}	25.16	30.0000	65.0000	30.0000	25.62	29.80	27.4484	67.8207	40.0000	23.81
P_{WG}	74.99	75.0000	75.0000	75.0000	75.00	74.95	73.2263	61.1047	75.0000	74.97
P_{TG3}	34.99	35.0000	33.9369	35.0000	35.00	34.91	45.0533	23.3276	35.0000	35.00
P_{SG}	59.99	50.0000	45.1813	50.0000	50.00	59.86	50.3881	46.9904	50.0000	60.00
P_{SHG}	40.35	45.5669	16.7919	45.5669	50.00	35.98	39.4714	33.1132	35.5868	41.66
V_1	1.060	1.0597	1.0639	1.0597	1.061	1.058	1.0521	1.0638	1.0610	1.062
V_2	1.055	1.0543	1.0600	1.0543	1.055	1.053	1.0479	1.0594	1.0560	1.057
V_5	1.045	1.0444	1.0479	1.0444	1.049	1.040	1.0402	1.0435	1.0455	74.97
V_8	1.049	1.0496	1.0498	1.0496	1.046	1.045	1.0476	1.0474	1.0497	35.00
V_{11}	1.096	1.1000	1.1000	1.1000	1.085	1.092	1.0581	1.1000	1.1000	60.00
V_{13}	1.063	1.0606	1.0536	1.0606	1.066	1.056	1.0568	1.0564	1.0571	41.66
Q_{TG1}	-0.89	-4.8064	-4.3041	-4.8052	-1.04	0.38	-7.7466	-4.9102	-4.6581	0.04
Q_{TG2}	14.43	6.9443	7.8094	6.9432	15.78	17.16	8.7748	8.7765	7.3152	17.27
Q_{WG}	24.34	20.5941	20.9463	20.5960	24.43	21.70	23.3476	21.7427	20.7149	25.02
Q_{TG3}	39.45	36.2915	37.4288	36.2921	40.00	39.23	44.3276	36.4820	36.6244	38.62
Q_{SG}	29.98	29.8880	29.1509	29.8884	25.00	29.96	17.3799	29.7941	29.8316	29.38
Q_{SHG}	20.41	18.6070	16.1932	18.6040	22.01	19.35	21.1666	16.9013	17.1485	17.51
F_{Loss}	2.0938	2.1669	2.5114	2.1669	2.2212	2.1244	2.1876	2.8962	2.1868	2.1059

Table 3.9: Comparison of statistical results of case 2 for different algorithms

Algorithms	**Minimum**	**Maximum**	**Average**	**Standard**
AEO	2.1244	2.1813	2.1452	3.14E – 02
GTO	2.2212	2.8313	2.4273	3.50E – 01
BMO **[5]**	2.1669	2.5209	2.1906	6.50E – 02
MFO **[5]**	2.1669	2.5215	2.2151	7.59E – 02
HS **[5]**	2.5114	2.6544	2.5789	3.90E – 02
GSA **[5]**	2.8962	4.3537	3.3340	3.59E – 01
PSO **[5]**	2.1868	3.8005	2.4511	3.05E – 01
BWOA **[5]**	2.1876	2.6771	2.4063	9.66E – 02
INFO	2.0938	2.1790	2.1047	1.87E – 02
CSBO	2.1059	2.1438	2.1221	8.70E-02

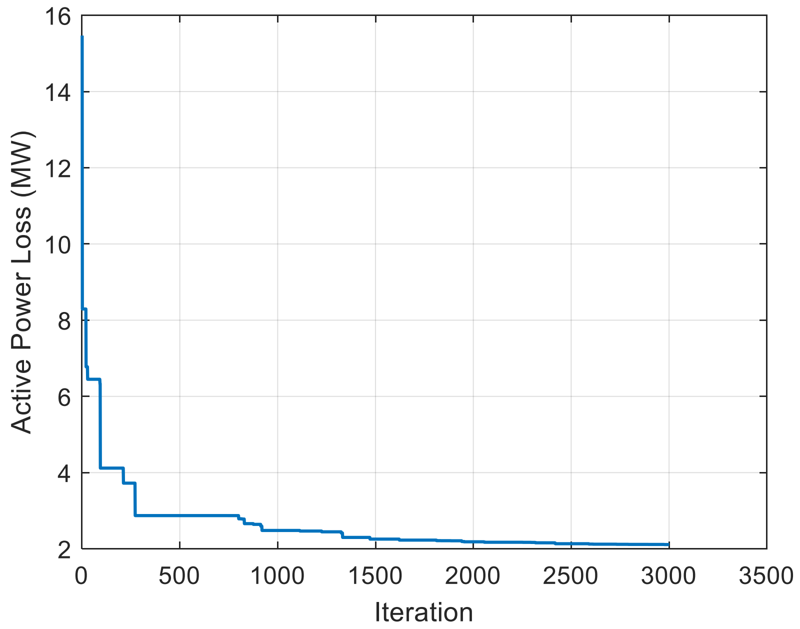

Figure 3-11**:** Convergence curve for OF in case 2

Case 3: Generation cost with emission minimization

The primary objective in this scenario is to minimize the generation cost while considering the impact of emissions. Reducing greenhouse gas emissions from conventional energy sources pose a significant challenge, and to address this, a carbon tax is imposed as a penalty. The goal is to optimize the generation cost while minimizing the environmental impact of emissions through the incorporation of this carbon tax.

Table 3.10 compares statistical results related to this case for different algorithms. Based on these results, the minimum value obtained by CSBO is 818.6050 $/h which is close to the minimum value obtained by BMO 820.4852 $/h as the difference is 1.8802 $/h. Nevertheless, the proposed algorithm has surpassed all other optimization techniques in terms of average, maximum, and standard deviation.

Table 3.10 : Comparison of statistical results of case 3 for different algorithms

Algorithms	Minimum	Maximum	Average	Std
INFO	820.56	822.08	821.19	4.13E – 01
AEO	820.58	821.85	821.46	5.27E – 01
GTO	821.75	822.66	822.25	3.37E – 01
BMO [5]	820.49	824.95	821.19	8.30E – 01
MFO [5]	820.81	825.89	821.34	9.90E – 01
HS [5]	827.02	827.78	827.67	2.07E – 02
GSA [5]	822.13	829.41	825.11	1.90E + 00
PSO [5]	820.81	835.15	824.55	3.34E + 00
BWOA [5]	822.58	826.82	824.44	1.11E + 00
CSBO	818.61	819.88	819.06	2.76E-01

Table 3.11 : Optimal results obtained of case 3 for different algorithms

Variable	**PSO**[5]	**GSA**[5]	**MFO**[5	**BMO**[5	**GTO**	**AEO**	**INFO**	**BWOA**	**HS**[5]	**CSBO**
P_{TG1}	126.595	127.043	126.593	126.69	126.42	127.21	126.63	126.0739	123.4563	126.20
P_{TG2}	44.2211	45.6540	44.2121	44.231	44.43	46.88	44.35	43.1541	65.0000	44.09
P_{WG}	48.4997	45.5324	48.5097	48.491	48.53	49.76	48.66	46.6268	43.4951	48.72
P_{TG3}	10.0000	14.3060	10.0000	10.000	10.00	10.00	10.01	12.7203	10.0000	10.05
P_{SG}	45.0261	40.7565	45.0261	45.026	45.33	41.38	45.52	44.8928	34.9329	41.88
P_{SHG}	14.4528	15.5839	14.4528	14.452	14.17	13.75	13.71	15.5858	12.4211	17.93
V_1	1.0816	1.0818	1.0816	1.0816	1.076	1.078	1.076	1.0587	1.0824	1.075
V_2	1.0682	1.0683	1.0681	1.0682	1.062	1.063	1.061	1.0437	1.0703	1.064
V_5	1.0466	1.0460	1.0466	1.0466	1.039	1.039	1.041	1.0353	1.0469	1.044
V_8	1.0488	1.0493	1.0488	1.0489	1.041	1.040	1.041	1.0359	1.0483	1.042
V_1	1.1000	1.1000	1.1000	1.1000	1.097	1.097	1.098	1.0587	1.1000	1.094
V_{13}	1.0536	1.0539	1.0536	1.0535	1.053	1.051	1.058	1.0437	1.0559	1.064
Q_{TG1}	-0.9694	-0.9707	-0.9946	-1.1055	4.93	5.08	5.10	-0.6057	-1.7444	-1.30
Q_{TG2}	13.7453	13.9367	13.7523	13.8389	19.25	22.26	15.50	-2.5917	14.5427	22.90
Q_{WG}	22.9881	23.2131	23.0018	23.0134	25.20	24.29	27.24	34.0173	23.9643	27.83
Q_{TG3}	37.1349	36.8448	37.1307	36.9844	39.24	37.53	39.20	48.5122	36.8996	37.11
Q_{SG}	28.6308	28.1882	28.6359	28.5148	30.00	29.98	29.84	19.9778	27.7266	27.70
Q_{SHG}	15.0950	14.9932	15.0995	15.2158	17.51	16.76	19.32	19.2986	15.8818	20.84
F_{CE}	820.806	822.131	820.807	820.485	821.749	820.5813	820.5593	822.5772	827.0182	818.6050

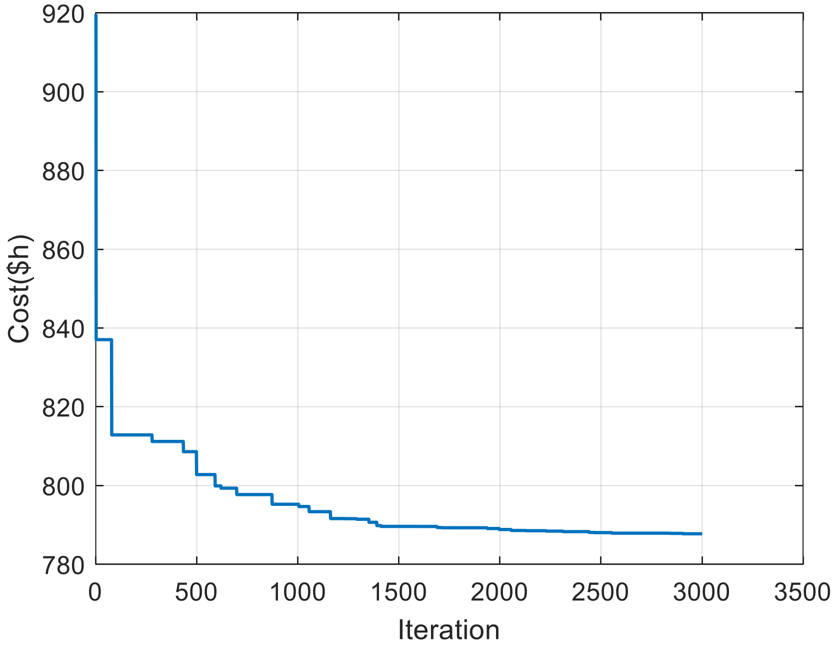

Figure 3-12 : Convergence curve for OF in case 3

The inclusion of a carbon tax incentivizes the use of renewable energy sources, which are clean and environmentally friendly. As a result, the electric power generation from these sources is expected to increase. In the first case, the active power produced from the solar generator was 40.66 MW. However, in the third case, when the carbon tax was imposed, the active power produced from the solar generator significantly increased to 41.88 MW, showing a notable increase of about 1.22 MW. We also notice the increase in both wind and combined solar PV with small hydro generator. This demonstrates the positive impact of the carbon tax in promoting the use of renewable energy and reducing greenhouse gas emissions.

The rest of study tested the performance of CSBO again, but with the modified IEEE 57-bus test system. The results obtained by the proposed algorithm were compared again with AEO and GTO, while BMO, MFO and PSO were selected from the rest of algorithms due to their efficiency. Combined solar PV and small hydro power generator are located at bus 6, while solar generator and wind generator are located at bus 9 and 12, respectively. The number of control variables to be minimized is 14 as mentioned in Table 3-13. Upper and lower bounds of control and state variables for modified IEEE 57-bus test system can be found Table 3-12

Table 3.12**:** Upper and lower bounds of control and state variables for test system I

	Control variables								State variables						
Variab	P_{TG1}	P_{TG2}	P_{TG3}	P_{TG4}	P_{SG}	P_{SHG}	P_{WG}	V_{gi}	Q_{TG1}	Q_{TG2}	Q_{TG3}	Q_{TG4}	Q_{SG}	Q_{SHG}	Q_{WG}
Min	0	0	0	0	0	0	0	0.95	-140	-17	-10	-140	-3	-8	-150
Max	575.88	100	140	550	220	100	210	1.1	200	50	60	200	9	25	155

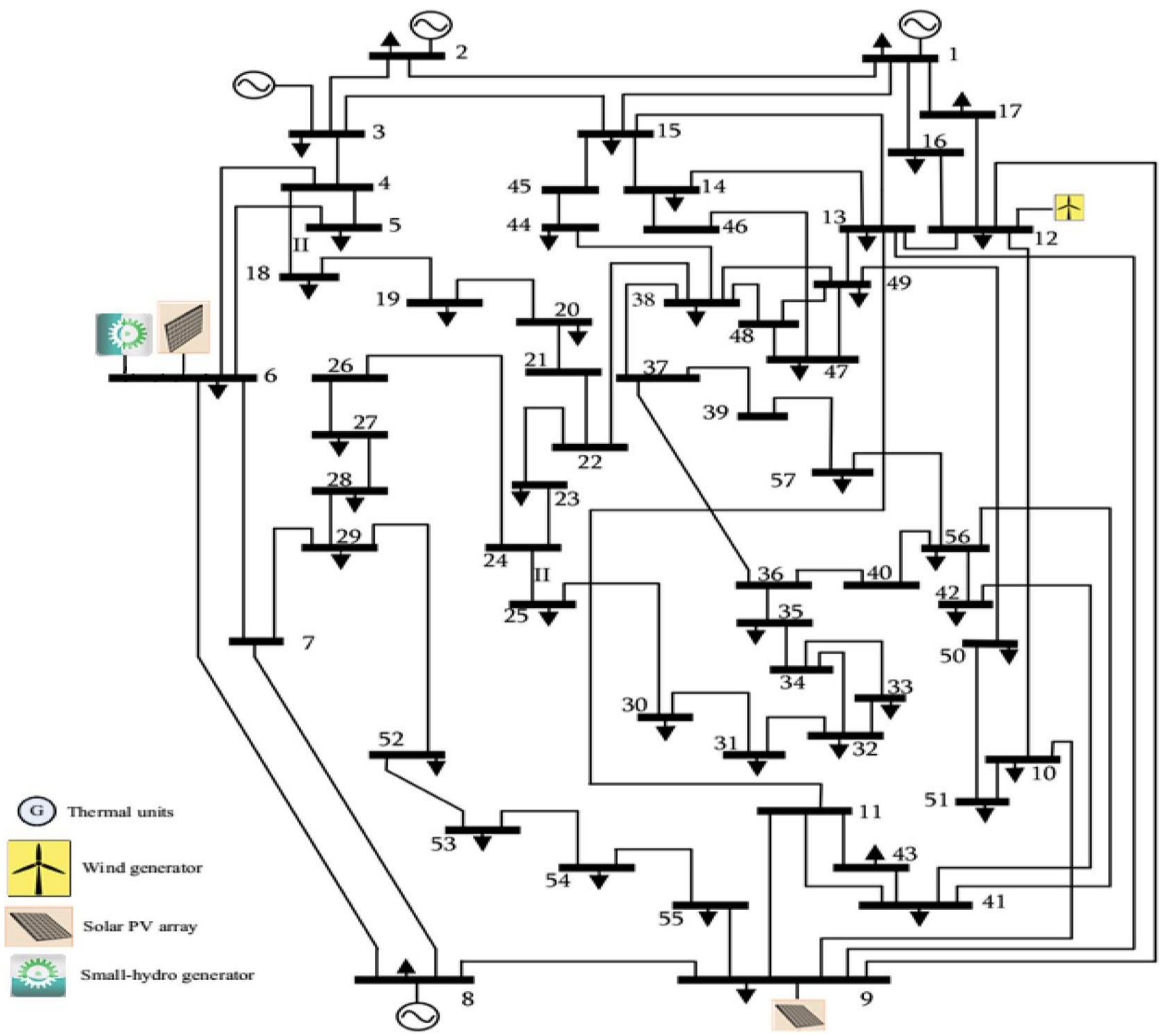

Figure 3-13 **:** Modified IEEE 57-bus-system [5]

Table 3-13 indicates the characteristics of the modified IEEE 57-bus test systems.

Elements	**IEEE 57-bus test system**
no. of buses	57
no. of transmission lines	88
no. of generators	07
no. of thermal generators	04
Number of renewable generators	03
no. of load buses	41
no. of control variables	14
Initial Real and reactive power demand	1250.80 MW ; 336.40 Mvar

Case 4: Total generation cost minimization

Table 3.14 showcases the optimal results obtained by CSBO and various other algorithms. The CSBO algorithm achieved a minimum total generation cost of 5256.7269 $/h, outperforming all other algorithms such as GTO (5260.0009 $/h), AEO (5260.2497 $/h), BMO (5300.457 $/h), MFO (5316.14 $/h), and PSO (5417.538 $/h). The difference between the value obtained by CSBO and the worst value obtained by PSO is 160.8111 $/h, resulting in significant cost savings of around 3856.4664 $ per day and 1408705.236 $ per year. It is worth noting that while GTO and AEO achieve results closer to CSBO, there is still a noticeable difference of 3.274 $/h or 28680.24 $ per year, indicating the superior performance of CSBO in terms of cost optimization. Figure 3-14 presents the convergence curve related to this case.

Table 3.14: Optimal results obtained of case 4 for different algorithms

Variables	MFO [5]	PSO[5]	AEO	INFO	BMO [5]	GTO	CSBO
P_{TG1}	554.2932	500.4827	556.88	556.81	555.5707	556.35	564.04
P_{TG2}	100	100	100.00	100.00	100	100.00	98.99
P_{TG3}	76.62421	140	76.62	76.61	76.62421	76.62	74.42
P_{SHG}	100	100	100.00	100.00	100	100.00	99.82
P_{TG4}	54.47699	38.48657	51.23	51.23	51.27178	51.68	48.78
P_{SG}	200	200	200.00	200.00	200	200.00	199.97
P_{WG}	210	210	210.00	210.00	210	210.00	209.73
V_1	1.1	1.1	1.051	1.067	1.1	1.059	1.069
V_2	0.95	1.1	1.043	1.055	1.1	1.048	1.055
V_3	1.1	0.95	1.020	1.019	0.95	1.014	1.022
V_6	0.95	1.1	1.014	1.015	1.024522	1.012	1.016
V_8	1.052336	1.015266	1.013	1.014	1.021023	1.016	1.020
V_9	1.1	1.1	0.985	0.984	0.95	0.987	0.987
V_{12}	0.958536	1.1	0.975	0.968	0.98036	0.976	0.962
Q_{TG1}	200	92.10943	98.26	143.76	200	125.02	159.13
Q_{TG2}	-17	50	50.00	49.99	50	49.98	39.44
Q_{TG3}	60	-10	48.70	27.89	-10	21.83	34.46
Q_{SHG}	-8	25	24.22	24.96	25	21.95	19.35
Q_{TG4}	179.9646	18.25645	109.32	113.89	106.2492	117.75	127.35
Q_{SG}	9	9	-1.48	-1.69	-3	-1.63	2.06
Q_{WG}	-46.2699	155	47.28	16.80	-1.47679	41.06	-2.08
F_{Cost} ($/h)	5316.14	5417.538	5260.2497	5259.2040	5300.457	5260.0009	**5256.7269**

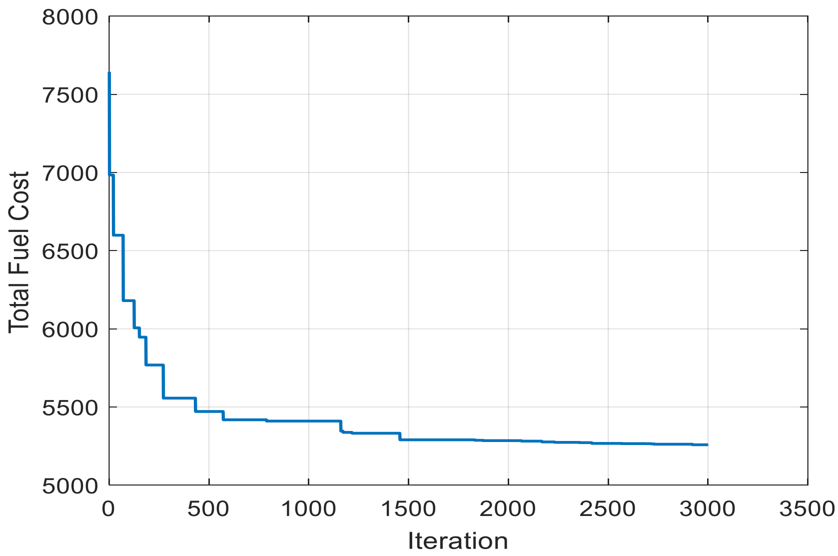

Figure 3-14 : Convergence curve for OF in case 4

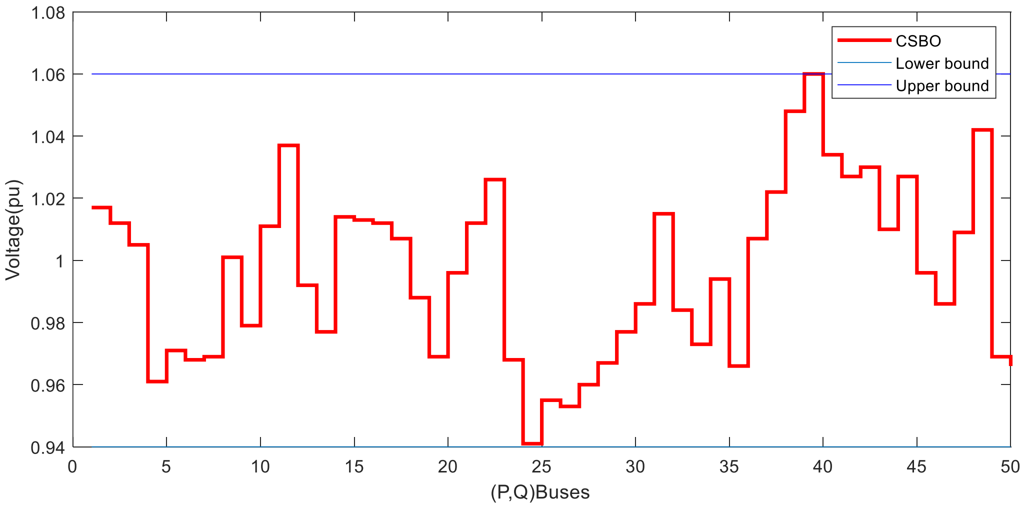

Figure 3-15 Voltage profiles in PQ buses of CSBO algorithm for case 4

Figure 3-15 represents Voltage profiles in PQ buses CSBO algorithm for case 4 The CSBO algorithm demonstrates its effectiveness in maintaining voltage profiles in PQ buses, as evident from the results. It showcases the algorithm's capability to ensure that the voltage constraints are respected and upheld.

Case 5: Total active power loss minimization

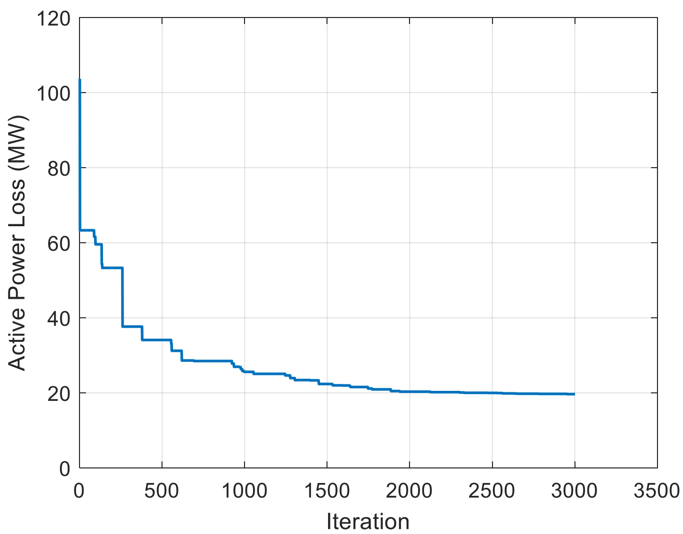

Figure 3-16: Convergence curve for OF in case 5.

The minimization of total active power loss is the secondary aim in the OPF problem using modified IEEE 57-bus test system. Again, the comparison of optimal results of CSBO with other different algorithms are illustrated in Table 3-15. Based on the results presented in this table, the minimum power loss of 19.6708 MW is obtained via CSBO. The proposed algorithm exceeds all optimization techniques, AEO (19.7633 MW), GTO (19.7703 MW), BMO (20.785 MW), MFO (21.3031 MW) and PSO (21.3621 MW). The convergence curve of total active power loss is depicted in Figure 3-1

Table 3.15: Optimal results obtained of case 5 for different algorithms

Variables	MFO [5]	PSO [5]	AEO	INFO	BMO [5]	GTO	CSBO
P_{TG1}	259.8313	273.4183	298.32	302.96	262.6827	293.00	291.90
P_{TG2}	39.25049	34.07384	0.99	3.32	39.12372	7.57	25.81
P_{TG3}	140	140	139.98	139.93	140	140.00	137.80
P_{SHG}	100	100	100.00	100.00	100	100.00	96.37
P_{TG4}	323.0214	314.67	321.26	314.31	319.7785	320.00	308.23
P_{SG}	200	200	200.00	200.00	200	200.00	200.00
P_{WG}	210	210	210.00	209.99	210	210.00	210.00
V_1	1.050806	1.0514	1.021	1.023	1.045745	1.021	1.041
V_2	1.1	1.1	1.014	1.015	1.1	1.013	1.033
V_3	1.1	1.1	1.016	1.017	1.1	1.010	1.031
V_6	1.1	1.1	1.025	1.022	1.1	1.021	1.026
V_8	1.030651	1.032615	1.038	1.029	1.03229	1.038	1.027
V_9	1.099932	0.95	1.003	0.999	0.95	1.005	1.004
V_{12}	0.950289	0.95	0.977	0.979	0.95768	0.981	0.995
Q_{TG1}	123.7601	123.7423	61.36	62.36	105.8136	63.65	72.53
Q_{TG2}	50	50	49.91	48.10	50	50.00	45.54
Q_{TG3}	60	60	31.10	35.75	60	17.62	39.49
Q_{SHG}	25	25	0.12	2.81	25	-4.14	3.14
Q_{TG4}	60.39987	71.64968	87.95	72.39	66.64419	91.72	49.50
Q_{SG}	9	-3	9.00	8.92	-3	9.00	4.93
Q_{WG}	-43.207	-42.0513	42.13	51.22	-21.5476	53.93	61.43
F_{Loss} (MW)	21.3031	21.3621	19.7633	19.7040	20.785	19.7703	19.6708

Case 6: Generation cost with emission minimization

Table 3.16 showcases the optimal results for the last case, which focuses on minimizing the generation cost while considering the emission effect. The CSBO algorithm achieved a minimum total generation cost of **5292.4087 $/h**, surpassing all other optimization algorithms including AEO (5298.1921 $/h), GTO (5299.6942 $/h), BMO (5320.851 $/h), PSO (5332.054 $/h), and MFO (5332.379 $/h). The difference between the value obtained by CSBO and the worst value obtained by MFO is 39.9703 $/h, resulting in significant cost savings of approximately 959.2872 $ per day and 350139.828 $ per year. It is worth noting that AEO and GTO achieve results close to CSBO, but there is still a noticeable difference of 5.7834 $/h or 50662.584 $ per year, highlighting the superior performance of CSBO in terms of cost optimization. Figure 3-17 presents the convergence curve related to this case.

Table 3.16**:** Optimal results obtained of case 6 for different algorithms

Variables	MFO [5]	PSO [5]	AEO	INFO	BMO [5]	GTO	CSBO
P_{TG1}	553.3165	554.1651	556.41	553.97	551.8909	554.41	558.16
P_{TG2}	100	100	99.17	100.00	100	100.00	99.99
P_{TG3}	76.62421	76.62421	76.63	76.55	76.6242	76.63	76.37
P_{SHG}	100	100	100.00	100.00	100	100.00	99.92
P_{TG4}	52.55224	51.77639	52.43	53.67	52.19387	53.44	50.88
P_{SG}	200	200	200.00	200.00	200	200.00	199.84
P_{WG}	210	210	210.00	210.00	210	210.00	210.00
V_1	1.078181	1.1	1.067	1.065	1.090978	1.046	1.054
V_2	1.1	0.95	1.056	1.053	1.1	1.038	1.040
V_3	1.036156	1.1	1.020	1.019	0.961542	1.016	1.006
V_6	1.1	1.1	1.008	1.014	1.1	1.012	1.005
V_8	1.011965	1.001535	1.018	1.013	1.044066	1.012	1.018
V_9	1.019763	1.1	0.988	0.985	0.95	0.989	0.991
V_{12}	0.985229	0.985591	0.964	0.968	1.1	0.979	0.983
Q_{TG1}	130.9053	200	146.51	138.29	65.39634	87.78	127.55
Q_{TG2}	50	-17	49.94	49.62	50	48.33	38.01
Q_{TG3}	42.54005	60	34.95	30.31	-10	45.12	12.35
Q_{SHG}	25	25	5.78	24.98	25	24.93	11.63
Q_{TG4}	78.66775	61.37461	126.76	109.10	63.4618	101.07	123.84
Q_{SG}	9	9	8.80	3.02	-3	9.00	5.46
Q_{WG}	27.21733	26.59974	3.09	18.53	155	59.21	59.53
F_{CE} ($/h)	5332.379	5332.054	5298.1921	5295.8597	5320.851	5299.6942	5292.4087

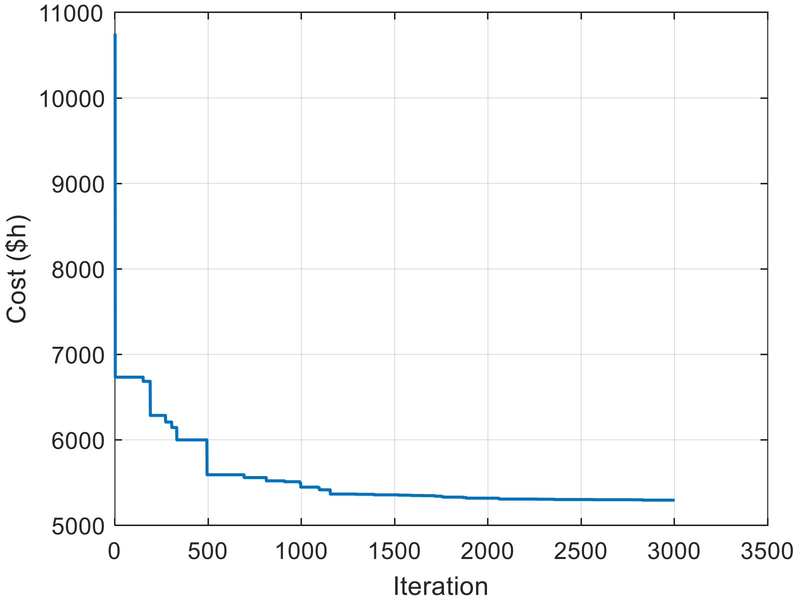

Figure 3-17**:** Convergence curve for OF in case 6

Conclusion

In this chapter, we introduced a novel algorithm called CSBO, designed specifically for solving the stochastic OPF problem in hybrid power systems. The algorithm was evaluated using three different single objective functions: minimizing total generation cost, total active power loss, and generation cost while considering emission effects. The objective was to find near-optimal solutions for these problems while ensuring compliance with equality and inequality constraints. The results obtained clearly demonstrate the superior performance of the CSBO algorithm in all cases compared to other algorithms such as AEO, BMO, GTO, MFO, INFO, and PSO. The CSBO algorithm consistently outperformed these algorithms, providing more effective and efficient solutions for the OPF problem in the considered scenarios.

General conclusion

GENERAL CONCLUSION

In conclusion, this thesis focused on addressing the optimal power flow (OPF) problem in hybrid power systems that incorporate renewable energy sources. The integration of these intermittent sources presents new challenges in optimizing power flow while considering operational, physical, and security constraints. To tackle these challenges, the Circulatory System-Based Optimization (CSBO) algorithm was applied as a metaheuristic approach inspired by the circulatory system. Through the application of the CSBO algorithm, this research demonstrated its effectiveness in solving the OPF problem in hybrid power systems. The algorithm consistently outperformed other optimization techniques, producing improved optimal costs for various objective functions.in case 1 the total generation cost reduction was 0.2% compared to INFO which is the closest result to CSBO and 1.65% for HS as the worst result this translates into 115425.264 $/year. Also, in case 4 we saw a 2.968% reduction compared to PSO resulting in significant cost savings of around 1408705.236 $ per year. This highlights the potential of metaheuristic algorithms in effectively integrating renewable energies into electrical networks. By incorporating probability density functions to model the uncertainty and variability of renewable sources, the thesis accounted for the intermittent nature of wind, solar, and small-hydro power generation. Two scenarios, overestimation, and underestimation, were considered to address the unpredictability of renewable energy sources, resulting in the inclusion of reserve cost and penalty cost in the generation cost.

The findings of this research contribute to the field by offering insights into the application of the CSBO algorithm specifically in the context of hybrid power systems. The successful utilization of CSBO highlights the importance of exploring novel metaheuristic approaches to overcome the limitations of traditional optimization methods.

Overall, this thesis demonstrates the potential of the CSBO algorithm in achieving effective and optimized power flow in hybrid power systems. The integration of renewable energy sources into the electrical grid can be enhanced through the utilization of advanced optimization techniques. This research contributes to the growing body of knowledge in the field of optimal power flow and provides a steppingstone for future research in improving the integration of renewable energies into electrical networks

REFERENCES

[1] A. M. Shaheen, R. A. El-Sehiemy, H. M. Hasanien, and A. R. Ginidi, “An improved heap optimization algorithm for efficient energy management based optimal power flow model,” *Energy*, vol. 250, p. 123795, 2022, doi: 10.1016/j.energy.2022.123795.

[2] M. Rawa *et al.*, “Economical-technical-environmental operation of power networks with wind-solar-hydropower generation using analytic hierarchy process and improved grey wolf algorithm,” *Ain Shams Eng. J.*, vol. 12, no. 3, pp. 2717–2734, 2021, doi: 10.1016/j.asej.2021.02.004.

[3] M. Herwan and Z. Mustaffa, “An application of improved salp swarm algorithm for optimal power flow solution considering stochastic solar power generation" e-Prime - Advances in Electrical Engineering , Electronics and Energy, *e-Prime - Adv. Electr. Eng. Electron. Energy*, vol. 5, no. June, p. 100195, 2023, doi: 10.1016/j.prime.2023.100195.

[4] Bouchekara, M. A. Abido, and M. Boucherma, “Optimal power flow using Teaching-Learning-Based Optimization technique,” *Electr. Power Syst. Res.*, vol. 114, pp. 49–59, 2014, doi: 10.1016/j.epsr.2014.03.032.

[5] M. H. Sulaiman and Z. Mustaffa, “Solving optimal power flow problem with stochastic wind–solar–small hydro power using barnacles mating optimizer,” *Control Eng. Pract.*, vol. 106, no. November 2020, p. 104672, 2021, doi: 10.1016/j.conengprac.2020.104672.

[6] P. P. Biswas, P. N. Suganthan, and G. A. J. Amaratunga, “Optimal power flow solutions incorporating stochastic wind and solar power,” *Energy Convers. Manag.*, vol. 148, pp. 1194–1207, 2017, doi: 10.1016/j.enconman.2017.06.071.

[7] CHAIB Ala Eddine.'étude de l'écoulement de puissance optimal par les méthodes d'optimisation metaheuristiques'.these de doctorat. (2021). Université des Frères Mentouri de Constantine 1

[8] BEN AMOR Riad et NAROURA Abderrahmane.' Optimisation de l’écoulement de puissance par une méthode métaheuristique (Big Bang-Big Crunch)'. Mémoire de Master. (2017). Université Echahid Hamma Lakhdar d'El Oued.

[9] BOUDAB Smail. 'application Des Reseaux De Neuronnes Dynamiques A L’optmisation De L’ecoulement De Puissance Dans Un Reseau Electrique' Memoire Magister. (2012). Université Larbi Ben M’hidi Oum El Bouaghi

[10] A. Mohamed and S. M. Lamine, “Contrôle optimal de l ’ écoulement de puissance dans un réseau I ntelligent en utilisant la méthode d ’ Optimiseur de troupes de gorilles (GTO)

Dédicaces," pp. 2020–2021, 2021.

[11] S. Mouassa, " Optimisation de l ' écoulement de puissance par une méthode métaheuristique (technique des abeilles en présence d'une source d'énergie renouvelable et systéme FACT)," 2012.Mémoire Magistère, Université Ferhat Abbas - Sétif-Algérie.

[12] J. D. Weber, "Implementation of a Newton-based Optimal Power Flow into a power system simulation environment," *Univ. Illinois*, vol. 2, p. 92, 1997.

[13] R. P. Singh, V. Mukherjee, and S. P. Ghoshal, "Particle swarm optimization with an aging leader and challengers algorithm for the solution of optimal power flow problem," *Appl. Soft Comput. J.*, vol. 40, pp. 161–177, 2016, doi: 10.1016/j.asoc.2015.11.027.

[14] M. R. AlRashidi and M. E. El-Hawary, "Hybrid particle swarm optimization approach for solving the discrete OPF problem considering the valve loading effects," *IEEE Trans. Power Syst.*, vol. 22, no. 4, pp. 2030–2038, 2007, doi: 10.1109/TPWRS.2007.907375.

[15] H. Abdi, S. D. Beigvand, and M. La Scala, "A review of optimal power flow studies applied to smart grids and microgrids," *Renew. Sustain. Energy Rev.*, vol. 71, no. May 2015, pp. 742–766, 2017, doi: 10.1016/j.rser.2016.12.102.

[16] K. Vaisakh, L. R. Srinivas, and K. Meah, "Genetic evolving ant direction particle swarm optimization algorithm for optimal power flow with non-smooth cost functions and statistical analysis," *Appl. Soft Comput. J.*, vol. 13, no. 12, pp. 4579–4593, 2013, doi: 10.1016/j.asoc.2013.07.002.

[17] "Development of an Efficient Calculation Method Based on Evolutionary Programming for Optimal Power Flow Considering Transient and Voltage Stabilities," no. December, 2009.

[18] R. R. Muhamadiev, N. A. Staroverova, and M. L. Shustrova, "Definition of neural network model for time series prediction," *J. Phys. Conf. Ser.*, vol. 2032, no. 1, 2021, doi: 10.1088/1742-6596/2032/1/012014.

[19] M. S. Osman, M. A. Abo-Sinna, and A. A. Mousa, "A solution to the optimal power flow using genetic algorithm," *Appl. Math. Comput.*, vol. 155, no. 2, pp. 391–405, 2004, doi: 10.1016/S0096-3003(03)00785-9.

[20] H. Bouchekara, "Solution of the optimal power flow problem considering security constraints using an improved chaotic electromagnetic field optimization algorithm," *Neural Comput. Appl.*, vol. 32, no. 7, pp. 2683–2703, 2020, doi: 10.1007/s00521-019-04298-3.

[21] P. M. Journals, "Palgrave Macmillan Journals, Operational Research Society," vol. 42, no. 8, pp. 673–683, 2016.

[22] G. M. Kakandikar and V. M. Nandedkar, "Sheet Metal Forming Optimization" Book, Engineering Optimization. 2018. doi: 10.4324/9781315156101-4.

[23] Z. Ma, G. Wu, P. N. Suganthan, A. Song, and Q. Luo, “Performance assessment and exhaustive listing of 500+ nature-inspired metaheuristic algorithms,” *Swarm Evol. Comput.*, vol. 77, no. January, 2023, doi: 10.1016/j.swevo.2023.101248.

[24] S. Mirjalili and A. Lewis, “The Whale Optimization Algorithm,” *Adv. Eng. Softw.*, vol. 95, pp. 51–67, 2016, doi: 10.1016/j.advengsoft.2016.01.008.

[25] S. Mirjalili, “Moth-flame optimization algorithm: A novel nature-inspired heuristic paradigm,” *Knowledge-Based Syst.*, vol. 89, no. July, pp. 228–249, 2015, doi: 10.1016/j.knosys.2015.07.006.

[26] M. Ghasemi *et al.*, “Circulatory System Based Optimization (CSBO): an expert multilevel biologically inspired meta-heuristic algorithm,” *Eng. Appl. Comput. Fluid Mech.*, vol. 16, no. 1, pp. 1483–1525, 2022, doi: 10.1080/19942060.2022.2098826.

[27] D. Freitas, L. G. Lopes, and F. Morgado-Dias, “Particle Swarm Optimisation: A historical review up to the current developments,” *Entropy*, vol. 22, no. 3, pp. 1–36, 2020, doi: 10.3390/E22030362.

[28] BEN HAMMOUDA Lahcen, “Minimisation des pertes actives dans un réseau électrique par l ’ algorithme d ’ optimisation par essaim de particules”,Mémoire Master. 2019. Université Kasdi Merbah Ouargla.

[29] V. Hayyolalam and A. A. Pourhaji Kazem, “Black Widow Optimization Algorithm: A novel meta-heuristic approach for solving engineering optimization problems,” *Eng. Appl. Artif. Intell.*, vol. 87, no. November 2018, p. 103249, 2020, doi: 10.1016/j.engappai.2019.103249.

[30] F. O. F. Technology, “Optimal power flow solution with non-conventional methods in smart grids,” no. June, 2021.

[31] I. U. Khan, N. Javaid, K. A. A. Gamage, C. James Taylor, S. Baig, and X. Ma, “Heuristic Algorithm Based Optimal Power Flow Model Incorporating Stochastic Renewable Energy Sources,” *IEEE Access*, vol. 8, pp. 148622–148643, 2020, doi: 10.1109/ACCESS.2020.3015473.

[32] Z. Ullah, S. Wang, J. Radosavljevic, and J. Lai, “A Solution to the Optimal Power Flow Problem Considering WT and PV Generation,” *IEEE Access*, vol. 7, pp. 46763–46772, 2019, doi: 10.1109/ACCESS.2019.2909561.

[33] P. P. Biswas, P. N. Suganthan, and G. A. J. Amaratunga, “Optimal power flow solutions incorporating stochastic wind and solar power,” *Energy Convers. Manag.*, vol. 148, pp. 1194–1207, 2017, doi: 10.1016/j.enconman.2017.06.071.

ABSTRACT

Abstract This thesis addresses the optimal power flow (OPF) problem in hybrid power systems involving renewable energy sources. The OPF problem includes optimizing various objectives while considering operational, physical, and security constraints. Traditional mathematical algorithms approaches have been used to solve the OPF problem, but they often suffer from limitations in terms of efficiency and convergence. To overcome the challenges introduced by intermittent RES, the Circulatory System-Based Optimization (CSBO) algorithm is proposed and applied on the Modified IEEE 30-bus and IEEE 57-bus test systems. Probability density functions (Weibull, lognormal and Gumbel) model the uncertainty of RESs. Two scenarios, overestimation and underestimation, account for intermittency by including reserve cost and penalty cost in the generation cost. The proficiency of the CSBO algorithm is validated by comparing its results with other optimizers. The research demonstrates that CSBO consistently outperforms other techniques, achieving improved optimal costs for various objective functions. This study contributes to the effective integration of renewable energies into electrical networks, enhancing economic and environmental benefits.

Key words: CSBO, Optimal power flow, hybrid renewable energy systems, Emission, Wind power, PV Solar power, small hydropower plant, Uncertainty.

Résumé : Cette thèse aborde le problème du l'écoulement de puissance optimal (OPF) dans les systèmes d'alimentation hybrides impliquant des sources d'énergie renouvelables. Le problème OPF comprend l'optimisation de divers objectifs tout en tenant compte des contraintes opérationnelles, physiques et de sécurité. Les approches traditionnelles d'algorithmes mathématiques ont été utilisées pour résoudre le problème de l'OPF, mais elles souffrent souvent de limitations en termes d'efficacité et de convergence. Pour surmonter les défis introduits par les SER intermittents, l'algorithme CSBO (Circulatory System-Based Optimisation) est proposé et appliqué sur les systèmes de test IEEE 30 bus modifiés et IEEE 57 bus. Les fonctions de densité de probabilité (Weibull, lognormal et Gumbel) modélisent l'incertitude des SER. Deux scénarios, la surestimation et la sous-estimation, tiennent compte de l'intermittence en incluant le coût de réserve et le coût de pénalité dans le coût de production. La compétence de l'algorithme CSBO est validée en comparant ses résultats avec d'autres optimiseurs. La recherche démontre que CSBO surpasse constamment les autres techniques, obtenant des coûts optimaux améliorés pour diverses fonctions objectives. Cette étude contribue à l'intégration efficace des énergies renouvelables dans les réseaux électriques, renforçant ainsi les avantages économiques et environnementaux

Mots Clés : l'écoulement de puissance optimal (EPO), Méthodes métaheuristiques, Optimisation par CSBO, Réseau électrique, énergie éolienne, Solaire photovoltaïque,

ملخص : تتناول هذه الأطروحة مشكلة تدفق الطاقة الأمثل (OPF) في أنظمة الطاقة الهجينة التي تنطوي على مصادر الطاقة المتجددة. تتضمن مشكلة OPF تحسين الأهداف المختلفة مع مراعاة القيود التشغيلية والمادية والأمنية. تم استخدام مناهج الخوارزميات الرياضية التقليدية لحل مشكلة OPF، لكنها غالبا ما تعاني من قيود من حيث الكفاءة والتقارب. للتغلب على التحديات التي أدخلتها التغيرات العشوائية لمصادر الطاقة المتجددة، تم اقتراح خوارزمية التحسين القائم على نظام الدورة الدموية (CSBO) وتطبيقها على أنظمة اختبار IEEE 30-bus و IEEE 57-bus المعدلة. تقوم دوال كثافة الاحتمال (Weibull وlognormal و Gumbel) بنمذجة عدم اليقين في مصادر الطاقة المتجددة. وهناك سيناريوان، هما المبالغة في التقدير والتقليل من التقدير، يمثلان التقطع بإدراج تكلفة الاحتياطي وتكلفة الغرامة في تكلفة التوليد. يتم التحقق من كفاءة خوارزمية CSBO من خلال مقارنة نتائجها مع المحسنات الأخرى. يوضح البحث أن CSBO يتفوق باستمرار على التقنيات الأخرى،

مما يحقق تكاليف مثالية محسنة لمختلف الوظائف الموضوعية. تساهم هذه الدراسة في التكامل الفعال للطاقات المتجددة في الشبكات الكهربائية، مما يعزز الفوائد الاقتصادية والبيئية.

الكلمات الرئيسية: تدفق الطاقة الأمثل، خوارزمية التحسين، التحسين بواسطة CSBO، الشبكة الكهربائية، طاقة الرياح، الطاقة الشمسية الكهروضوئية.